also a maternally expressed imprinted gene at the embryonic stage, especially in extraembryonic tissues.

The three *Pon* genes are located adjacent to each other on mouse chromosome 6 and human chromosome 7 (Fig. 1A; Primo-Parmo et al. 1996). Human PON1, PON2, and PON3 share 65% similarity at the amino acid level. PON1 is an enzyme associated with high-density lipoprotein (HDL) that is believed to protect against the early events of atherogenesis via its ability to hydrolyze oxidized phospholipids. It is also involved in the detoxification of organophosphate insecticides, such as parathion and chlorpyrifos. In contrast, PON2 and PON3 lack paraoxonase activity, although they have similar antioxidant properties. PON3 is also found in HDL, whereas PON2 is not associated with HDL (Davies et al. 1996; Shih et al. 1998; Draganov et al. 2000; Ng et al. 2001).

As shown in Figure 4A, *Pon1* expression was detected mainly in liver and lung. Therefore, we tested the imprinting status of *Pon1* in liver and lung from neonates. As shown in Figure 4B, the same biallelic expression pattern of *Pon1* was observed between reciprocal F_1 crosses, although it is apparent that the expression of the JF1 allele was constantly higher than that of the B6 allele in both tissues. It has been reported that DNA polymorphisms in human promoter regions affect the levels of *IL-4* and *TNF-α* expression (Song et al. 1996; Wilson et al. 1997). Therefore, it is highly possible that genes showing strain-specific (or strain-biased) expression exist in the mouse. In this experiment, apparent allele-biased expression was also observed in *Pon2* and *Pon3* (see following). To distinguish imprinted parental allele-specific expression from strain-specific expression, it is very important to analyze the imprinting status in the F_1 of both crosses. It was difficult to obtain reliable results from embryos, placentas, and yolk sacs because of low expression of *Pon1* in these tissues (data not shown). Mouse *Pon2* is ubiquitously expressed (Fig. 4A) and biallelic expression was observed in neonatal brain (Fig. 4C, right-hand lanes) and other neonatal tissues (skeletal muscle, spleen, kidney, liver, and lung; data not shown). However, significant maternally biased expression was observed in day 10 placenta (3.5 and 4.0) and to a lesser degree in day 13 yolk sac samples (1.9 and 2.0) in (B6 × JF1) F_1 and (JF1 × B6) F_1, respectively (Fig. 4C). Therefore, *Pon2* is imprinted, at least, in these restricted tissues at the embryonic stages.

As shown in Figure 4A, mouse *Pon3* is expressed mainly in liver and lung in the adult. There was no evidence of its imprinting in neonatal liver and lung (Fig. 4D, right-hand lanes). However, *Pon3* showed maternally biased expression in day 10 placenta and day 13 yolk sac samples, because the B6 (534 bp) and JF1 (727 bp) alleles went up and down reciprocally in these tissues of two different F_1s (Fig. 4D). Similar maternal biases were also observed in day 10 embryo to a lesser degree. It was also evident that the expression of B6 alleles in embryo, placenta, and yolk sac was much higher than that of JF1 alleles in both reciprocal F_1s. Therefore, M/P values are not a good indicator of imprinting in this case.

DISCUSSION

In this study, we demonstrated that at least two paternally expressed genes and four maternally expressed genes are located in a 1-Mb region between *Col1a2* and *Asb4* in the mouse proximal chromosome 6 and form a large cluster of imprinted genes. Of these, *Sgce* and *Peg10* show paternal expression in an all-or-none fashion, and *Asb4* shows mainly maternal expression with a lesser paternal contribution (Piras et al. 2000; Mizuno et al. 2002). One characteristic of this cluster is that three genes (*Neurabin*, *Pon2*, and *Pon3*) show preferential maternal expression in the embryonic stage. They show biallelic expression in neonatal tissues, but their expression in extraembryonic tissues appears maternally biased. Although most imprinted genes identified so far show clear all-or-none monoallelic expression patterns, some imprinted genes showing weak parental preferences were recently reported, including *Tnfrh1* on mouse distal chromosome 7 and *Dio3* on mouse distal chromosome 12 (Clark et al. 2002; Tsai et al. 2002). The former shows a weak maternal bias in several organs and the latter shows preferential paternal expression in embryos and placentas to differing degrees. It is rational to expect that genes showing differential expression of paternal and maternal alleles that are always associated with the same parental biases be classified as imprinted genes.

What is the mechanism of this preferential expression? There are three possibilities: (1) the existence of overlapping transcripts from other gene(s) showing paternal or biallelic expression; (2) the existence of two promoters, one for maternal expression and the other for biallelic expression; and (3) the relaxation of genomic imprinting: the change from an imprinted state to a nonimprinted state occurs in certain situations.

The first possibility, overlapping RNA, such as readthrough products of *Peg10*, can be excluded, because no other cDNA bands of different sizes or genomic DNA bands of the same size were detected in RT-PCR experiments for *Pon1* and *Pon2*, when the two primers were located in different exons. The amplified bands were directly sequenced to confirm that they were derived from the genes in question, as mentioned. Moreover, as far as the expression profile of *Peg10*

Figure 2 *Peg10* imprinted expression associated with primary DMR. (*A*) The genomic structure of *Peg10* and bisulfite sequencing analyses of the *Peg10* repeated sequence region. The full-length *Peg10* sequence was determined by 5′-RACE analysis. The white boxes are untranslated regions and putative open reading frames are shown with black boxes. Two putative ORFs of *Peg10* are shown in gray boxes below; ORF1 shares 30% amino acid identity with the gag protein, and ORF2 predicted from a −1 frameshift of ORF1 shares 25% identity with the pol protein of Sushi-ichi retrotransposon, respectively. The translational frameshifting of ORF1–ORF2 is commonly observed in retroviruses and gypsy-type LTR retrotransposons. The arrows indicate the 5′–3′ direction of *Peg10* and *Sgce*. The DNA methylation status of *Peg10* repeats in day 10 embryo, eggs, and sperm are shown. Differential methylation was observed in the day 10 embryo as well as the day 10 placenta (data not shown). DNA polymorphisms between JF1 and B6 were used to distinguish parental alleles. The entire *Peg10-Sgce* CpG island indicated by gray lollipops shows a differentially methylated status similar to that in the *Peg10* repeats (data not shown). (*B*) Twelve *Peg10* intronic 29-bp repeat sequences. Shaded boxes indicate homology with the most frequent sequence, GCGCTTCATGCGCTACAAAATACTCATAG (four times). (*C*) Northern blot profiles of *Peg 10* in mouse adult tissues. Total RNA from mouse adult brain (lane *1*), heart (lane *2*), lung (lane *3*), liver (lane *4*), spleen (lane *5*), kidney (lane *6*), stomach (lane *7*), small intestine (lane *8*), skeletal muscle (lane *9*), skin (lane *10*), thymus (lane *11*), testis (lane *12*), uterus (lane *13*), and placenta (lane *14*) was analyzed. Ribosomal RNA detected by ethidium bromide (EtBr) staining was used as a marker. Strong *Peg10* expression was observed only in placenta, and the major transcript was estimated to be ~6.5 kb long. (*D*) Paternal expression of *Peg10*. Paternal expression of *Peg10* in day 10 embryo, placenta, yolk sac, and neonatal brain is demonstrated by direct sequencing of the RT-PCR products, by comparing the sequence profiles of genomic DNA containing B6 and JF1 alleles equally.

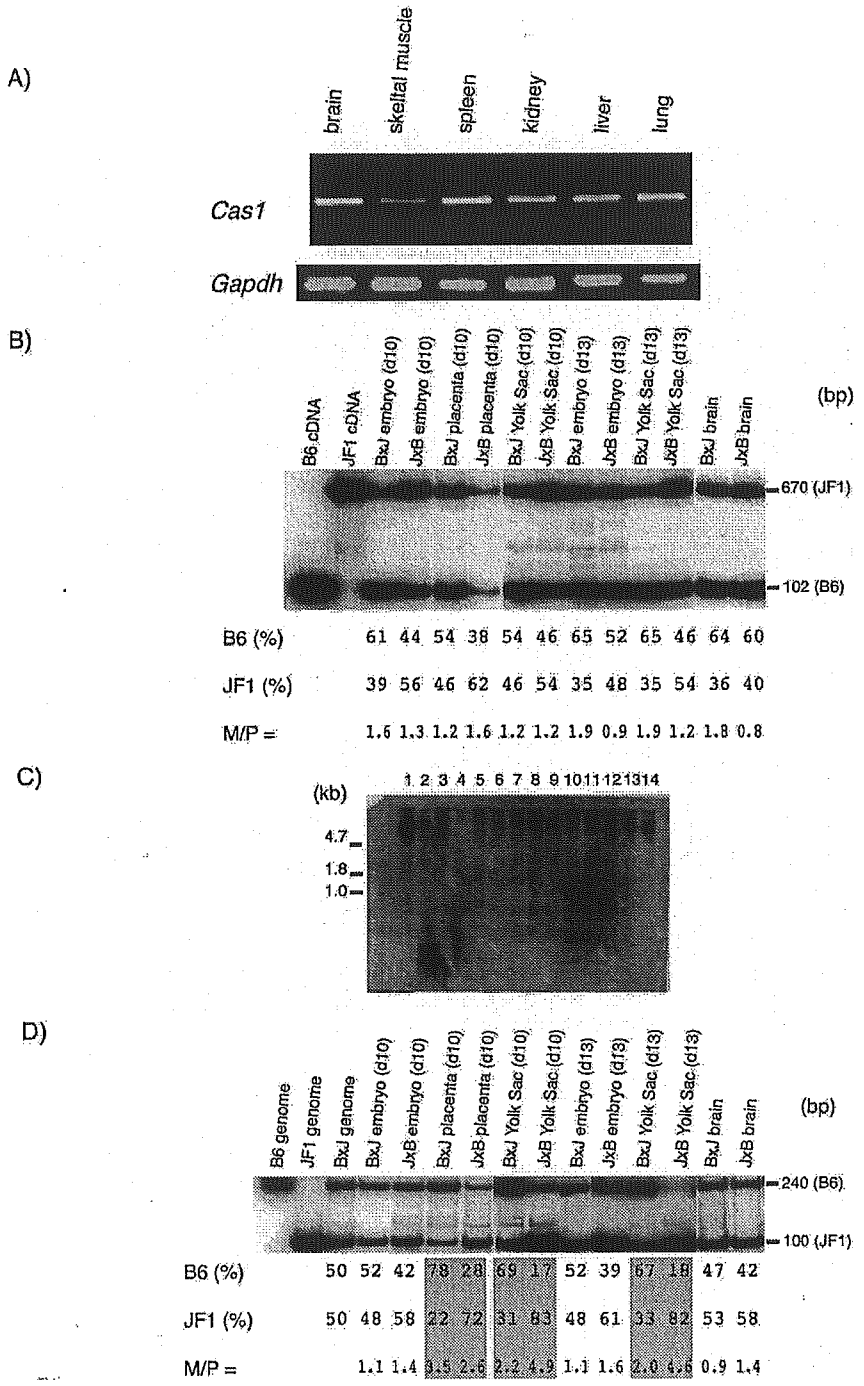

Figure 3 Characterization of *Cas1* and *Neurabin*. (*A*) Expression profiles of *Cas1*. The RT-PCR products (30 cycles for *Cas1* and 25 cycles for the control *Gapdh*) using total RNA from a range of adult tissues (brain, skeletal muscle, spleen, kidney, liver, and lung) are shown. (*B*) *Cas1* expression in the embryonic stage. In the *DdeI* RFLP experiment combined with Hot-stop PCR using a radioisotope-labeled primer, the B6 and JF1 alleles yielded 102- and 670-bp fragments, respectively. Three experiments were carried out in the same samples and the average ratios between the B6 and JF1 alleles, and also between maternal and paternal alleles (M/P values), are shown below. Similar results were obtained in the tissues from different individuals (data not shown). (*C*) Northern blot profiles of *Neurabin* in mouse adult tissues. Strong expression is observed in the brain sample, whereas weak ubiquitous expression is observed in all other tissues. (*D*) Maternal expression of *Neurabin*. In the *AciI* RFLP analysis with Hot-stop PCR, the B6 and JF1 alleles yielded 240- and 100-bp fragments, respectively. Preferential maternal expression was observed in placenta (day 10) and yolk sac (day 10 and 13) samples. The gray boxes indicate clear maternal biases in reciprocal crosses.

is concerned, this hypothesis is unlikely, because *Peg10* is strongly expressed only in placentas, where the maternal preferential expression of these genes was observed; the genes showed completely biallelic expression in neonatal tissues, where *Peg10* expression is very low.

The second possibility is more likely, because several EST clones possessing different transcription start sites for *Neurabin* have been registered in GenBank (accession no. AW048064, BB617696, and BB639924). There are also several examples in which different promoters show different expression profiles depending on tissue and developmental stage. These include *Igf2* and human *PEG1/MEST* (paternal and biallelic), *Gnas*, *Nesp*, and *GnasXL* (paternal, maternal, and biallelic) and mouse *Meg1/Grb10* (maternal and paternal) and human *GRB10* (biallelic and paternal; Vu and Hoffman 1994; Peters et al. 1999; Kosaki et al. 2000; Li et al., 2000; Kobayashi et al., 2001; Hikichi et al. 2003). In such cases, intermediate types of expression should be observed where two different transcripts overlap. Further analyses to identify the precise promoters of these genes will be necessary to test this possibility.

It is also worth considering the third possibility, the relaxation of imprinting, because there is evidence for a change in the expression of imprinted genes associated with a change in DNA methylation in DMR regions in some diseases and cancers as a result of mutation or deletions. However, we do not know of a mechanism that relaxes imprinting functions in normal development without changes in DNA sequences.

In conclusion, the maternal bias in expression should be reflected by some imprinting-related mechanism, overlapping transcripts from different promoters showing different parental expression profiles, or the relaxation of imprinting.

There are two conserved imprinted regions in the mouse proximal chromosome 6 and the human syntenic region of the long arm of chromosome 7. In the mouse, the *Peg1/Mest* region is responsible for perinatal growth retardation, and the region examined in this work is responsible for early embryonic lethality when maternal duplication occurs. However, human maternal disomy of the chromosome 7 containing both imprinted regions is associated with the perinatal growth retardation known as Silver-Russell syndrome, but there is no evidence of early embryonic lethality (Preece et al. 1997). Therefore, two questions arise concerning the latter imprinted region: what gene(s) is responsible for early embryonic lethality in the mouse and why is no severe lethal phenotype observed in humans?

One simple possibility is the existence of a mouse-specific imprinted gene(s) that causes early embryonic lethality. We have confirmed that both human *PEG10* and mouse *Peg10* are paternally expressed in an all-or-none manner. It has been reported that a mutation in human *SGCE* on chromosome 7q21 causes myoclonic dystonia (OMIM no.159900), which is characterized by bilateral, alcohol-sensitive myoclonic jerks involving mainly the arms and axial muscles (Zimprich et al. 2001). The family trees of patients show paternal inheritance of this disease, indicating that human *SGCE* is also a paternally expressed gene. However, it is not known whether it shows completely monoallelic expression, as with mouse *Sgce*, or paternal expression with a maternal contribution. The imprinting status of the other four human homologs corresponding to the mouse maternally expressed genes, *Neurabin*, *Pon2*, *Pon3*, and *Asb4*, is not known. Therefore, analyses of these human homologs are required to elucidate phenotype differences between the human and mouse. In this study, we analyzed genes in a 1-Mb region near *Sgce* and *Asb4*. It is also probable that there are other imprinted genes responsible for the mouse lethal phenotype downstream from *Asb4*.

Another explanation for the human–mouse phenotype discrepancy is the difference in the mechanisms producing human uniparental disomies and mouse uniparental duplications. It has been reported that some human chromosomal disomies arise from trisomies, because congenital chromosome mosaicism showing trisomy in placentas containing both paternal and maternal alleles is sometimes observed in human uniparental disomy patients. In contrast, mice with maternal duplication have been constructed by mating mice with Robertsonian translocations or reciprocal translocations at the same locus (see http://www.mgu.har.mrc.ac.uk/imprinting/imprinting.html). Consequently, all the tissues in the embryos and placentas possess two maternal alleles for the duplicated regions. Therefore, it is possible that the mouse early embryonic phenotype results from a placental abnormality, which is not apparent in the human case. In this case, *Sgce* and *Peg10* are most likely involved, because they show complete paternal expression and are strongly expressed in placentas. Gene targeting approaches to these genes are necessary to test this possibility.

In this report, we identified a primary DMR in the region where the first exons of *Sgce* and *Peg10* overlap. Twelve repeat sequences of a 29-bp fragment are located within a CGI just downstream from the *Peg10* first exon. It would be very interesting to determine whether this DMR regulates only the two paternally expressed genes or all the genes in the cluster, including the maternally expressed genes, because there are no apparent DMRs in this region. A gene-targeting study of the DMR will be very important for elucidating the mechanism regulating this imprinted region in mouse proximal chromosome 6.

METHODS

Identification of Genes and CGIs From a 1-Mb Region Between *Col1a2* and *Asb4*

The genomic sequence in the 1-Mb region between Mb 1.2 and 2.2 of *Mus musculus* WGS supercontig Mm6_WIFeb01_97 (GenBank accession no. NW_000272) containing *Sgce* and *Asb4* was repeat-masked using Repeat Masker, and then used in a BLASTN search of dbESTs to identify transcripts. Five of the identified EST clusters were identical to mouse *Col1a2* (GenBank accession no. NM_007743), *Sgce* (NM_011360), *Pon1* (NM_011134), *Pon2* (NM_008896), *Pon3* (NM_008897), and *Asb4* (NM_023048), and the rest were orthologs of human *Cas1* (NM_022900), *PEG10* (NM_015068), and rat *Neurabin* (NM_053473). The mouse gene sequences (registered as *Peg10*: AB091827, *Neurabin*: AB091828, and *Cas1*: AB091829) were confirmed using RT-PCR and nucleotide sequencing. To identify CGIs, we ran the program Cpgplot (http://www.ebi.ac.uk/emboss/cpgplot/) with the following parameters: Observed/Expected ratio > 0.60, Percent C + Percent G > 50.00, Length > 300. Four CGIs were identified: *Cas1* CGI (1304815bp-1305668bp; NW_000272), *Peg10-Sgce* CGI (1453104bp-1453415bp; NW_000272), *Neurabin* CGI (1609519bp-1610544bp; NW_000272), and *Pon2* CGI (2009459bp-2010036bp; NW_000272) corresponding to the promoter regions of these genes.

RT-PCR and 5′-RACE

Genomic DNA and total RNA were prepared from several tissues from the F_1 of (B6 × JF1), (JF1 × B6), and (B6 × C3H)

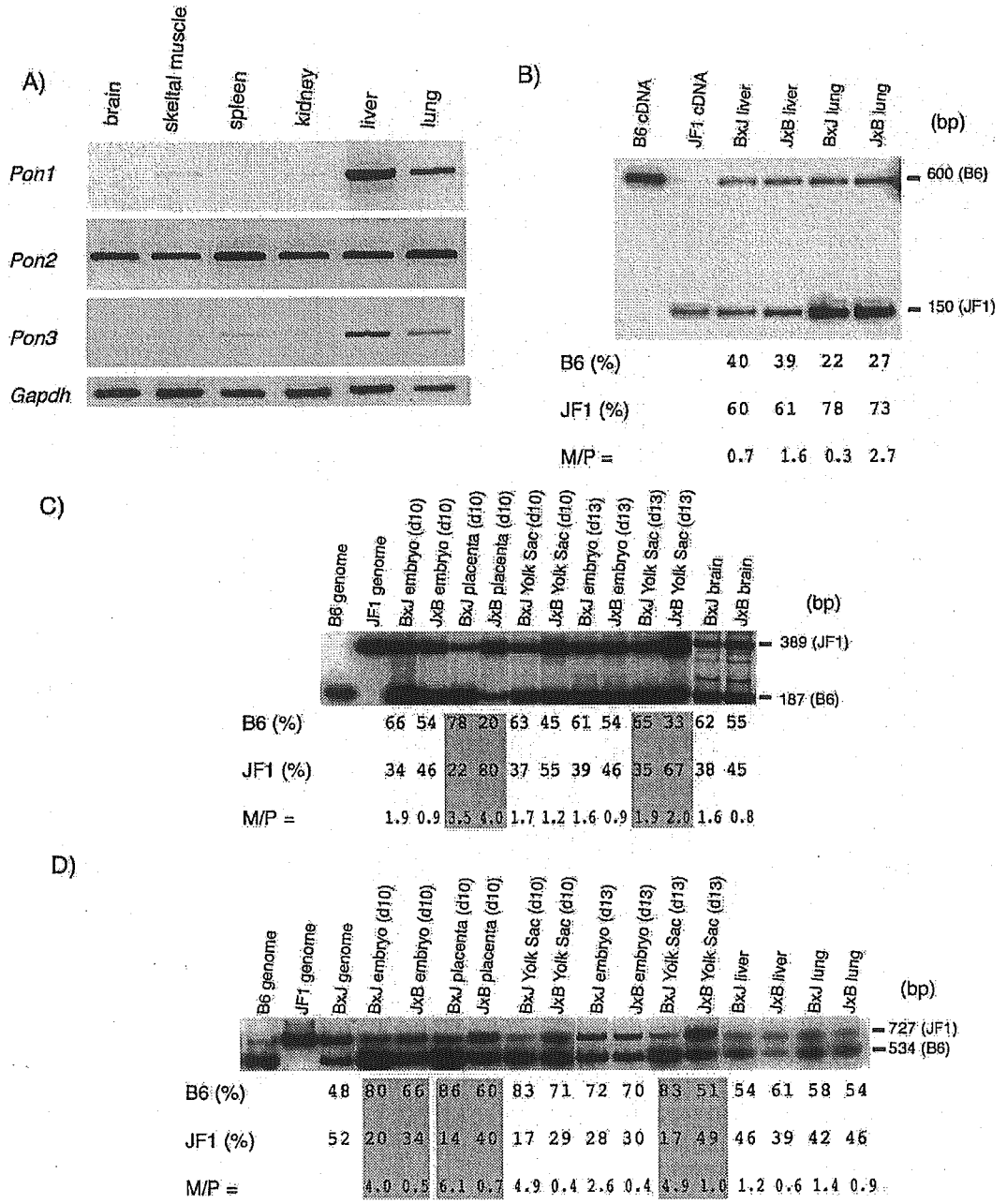

Figure 4 Characterization of *Pon1*, *Pon2*, and *Pon3*. (*A*) Expression profiles of *Pon1*, *Pon2*, and *Pon3*. RT-PCR products (30 cycles for *Pon1*, *Pon2*, and *Pon3*, and 25 cycles for *Gapdh*) from the same adult tissues used in Fig. 3A are shown. *Pon2* was expressed ubiquitously, whereas *Pon1* and *Pon3* expression were observed mainly in liver and lung. (*B*) Biallelic expression of *Pon1*. In the *Msp*I RFLP experiment with Hot-stop PCR, the B6 and JF1 alleles yielded 600- and 150-bp fragments, respectively. The biallelic expression patterns were unchanged between reciprocal crosses, although JF1 alleles were always expressed more strongly than B6 alleles. (*C*) Maternal expression of *Pon2*. In the *Hae*III RFLP experiment with Hot-stop PCR, the B6 and JF1 alleles yielded 187-bp and 389-bp fragments, respectively. Preferential maternal expression of *Pon2* was observed in placenta and to a lesser degree in day 13 yolk sac. (*D*) Maternal expression of *Pon3*. In the *Ple*I RFLP experiment with Hot-stop PCR, the B6 and JF1 alleles yielded 534-bp and 727-bp fragments, respectively. Maternal biases of both the B6 and JF1 alleles were observed in day 10 placenta and day 13 yolk sac and also observed in day 10 embryo to a lesser degree. Note that the B6 allele was expressed more strongly than the JF1 allele in all cases.

mice, using ISOGEN (Nippon Gene), as described previously (Kaneko-Ishino et al. 1995). cDNA was synthesized from 1 μg of total RNA using Superscript II reverse transcriptase (Life Technologies) with an oligodT primer. Gene expression profiles were deduced by agarose gel electrophoresis of RT-PCR products with ethidium bromide (EtBr) staining. The primers used for the expression profiles were the same as those described in the next section. A SMART RACE cDNA Amplification Kit (Clontech) was used for 5′-RACE, following the manufacturer's protocol. RNA was prepared from B6 day 16 embryos, and the gene-specific primer used was GSP: 5′-GTGAGAGGGGCTTCACTCCCCTG -3′. The amplified DNA fragments were purified and sequenced directly.

Allelic Analysis of Gene Expression Combined With Hot-Stop PCR

DNA polymorphisms in six genes between JF1 and C57BL/6 were detected in restriction fragment length polymorphism (RFLP) and single site polymorphism (SSP) analyses. For RT-PCR, 10 ng of cDNA in a 100-μL reaction mixture containing 1× ExTaq buffer (TaKaRa), 2.5 mM dNTP mixture, primers, and 2.5 U of ExTaq (TaKaRa) was subjected to 30–35 PCR cycles. In the case of *Pon3*, we performed nested PCR and added 10 PCR cycles in the second amplification. PCR was carried out on a Perkin Elmer GeneAmp PCR system 2400 under the following cycle conditions: 96°C for 15 sec, 65°C for 30 sec, and 72°C for 30 sec. The final cycle of PCR was performed in the presence of a primer labeled with [γ-^{32}P] ATP. The PCR product was digested with the appropriate restriction endonuclease and electrophoresed on a 10% polyacrylamide gel. The intensity of the PCR products was measured with a BAS2000 Bioimaging Analyzer (Fuji Film). Experiments were carried out three times and average ratios were shown. Errors in observed values were within 5% in all cases except J × B yolk sac (day 13) of *Cas1*. The following primers were used for DNA amplification: *Cas1*, 5′-AGCAGAGTGTAACGAACTCCAC-3′ and 5′-CACAGTGGAC GGGTGAATGTGC-3′ *; *Neurabin*, 5′-ACTCTCCTGCCGAG GCTG-3′ and 5′-CAGTTTCAGGGGCTCTCACT-3′ *; *Peg10*, 5′-GGGTAGATAATCATAAGTATTTTGGGC-3′ and 5′-CAACATTCTAAACTTTATTCCAGCAAC-3′; *Pon1*, 5′-ACAAGAACCATCGGTCTTCC-3′ * and 5′-CCTTCTGCTAC CACCTGGAC-3′; *Pon2*, 5′-ACGAGCTCCTTCCAAGTGTG-3′ and 5′-ACCTCTGATGCAGGAGGATG-3′ *; *Pon3* (the first amplificaton), 5′-TCAGAAGTACTACGCATCCAGG-3′ and5′-CATGGCTGAAGGTAACTGTCC-3′; *Pon3* (the second amplification), 5′-GAACAACGGCTCTGTGCTTC-3′ * and 5′-ATGCACCAAGCTAGCTGATG-3′. Asterisks indicate labeled primers with [γ-^{32}P] ATP used in the last PCR cycles.

For RFLP analysis of *Cas1*, *Neurabin*, *Pon1*, *Pon2*, and *Pon3*, the PCR products were digested with *Dde*I, *Aci*I, *Msp*I, *Hae*III, and *Ple*I. For SSP analysis of *Peg10*, the PCR product was sequenced on an ABI 3100 sequencer using Big-Dye terminator chemistry (Applied Biosystems).

Methylation Analyses of Embryos, Placentas, Eggs, and Sperm

Genomic DNA and RNA were isolated from both day 10 embryos and placentas, as well as eggs and sperm, using ISOGEN, as described in the RT-PCR section. Purified genomic DNA was treated with a sodium bisulfite solution, as described previously (Raizis et al. 1995). During this process, cytosine was converted to uracil, except methylated cytosine. The sodium bisulfite-treated DNA was amplified with following the primers: *Peg10-Sgce* CGI, 5′-GTAAAGTGATTGGTTTTGTATTTTTAA GTG-3′ and 5′-TTAATTACTCTCCTACAACTTTCCAAATT-3′; *Cas1* CGI, 5′-GTTTAGGTAGTTGTTAGTTTATTTGGGTA TAG-3′ and 5′-CCTCCCTAATAACCTCCTACCTTAATAAC-3′; *Neurabin* CGI, 5′-GGTGTTTTTTGGTATTAGGTTAGATTG-3′ and 5′-ATAAACACCCTCCCCTCTCC-3′; *Pon2* CGI, 5′-AGTGTTTAGGTTTTGGTGGAAGTG-3′ and 5′-CCCAAACTT AACTAAATTAAAAAAACTCC-3′.

The DNA fragments were amplified using ExTaq (TaKaRa) for 35–40 cycles under the following cycle conditions: 96°C for 15 sec, 60°C for 30 sec, and 72°C for 1 min. The amplified fragments were cloned into plasmids and sequenced. DNA polymorphisms in *Peg10* promoter region (T/A; B6/JF1;1453020 bp; NW_000272) and DNA polymorphisms in *Cas1* promoter region (A/G; B6/JF1;1304769 bp; NW_000272) and in *Pon2* promoter region (T/G; B6/JF1; 2009669 bp; NW_000272) were used to determine paternal and maternal alleles of *Cas1* CGI and *Pon2* CGI, respectively.

Northern Blot Analysis

To analyze *Peg10* and *Neurabin* expression, we used membranes of numerous adult tissues in Northern blot (Seegene, Korea) experiments. The 3′ part of *Peg10* was amplified with primers 5′-GGGTAGATAATCATAAGTATTTTGGGC-3′ and 5′-CAACATTCTAAACTTTATTCCAGCAAC-3′ and *Neurabin* was amplified with primers 5′-ACTCTCCTGCCGAGGCTG-3′ and 5′-CAGTTTCAGGGGCTCTCACT-3′, and used as a DNA probe. Hybridization was performed at 42°C in Ultrasensitive Hybridization Buffer (Ambion) for 18 h. The membrane was then washed with a solution containing SSC and 0.1% SDS at 42°C to a final stringency of 0.1 × SSC.

ACKNOWLEDGMENTS

This work was supported by grants from CREST, the research program of the Japan Science and Technology Cooperation (JST), Asahi Glass Foundation, Uehara Memorial Life Science Foundation and the Ministry of Health, Labour for Child Health and Development (14-C) to F.I.

The publication costs of this article were defrayed in part by payment of page charges. This article must therefore be hereby marked "advertisement" in accordance with 18 USC Section 1734 solely to indicate this fact.

REFERENCES

Beechey, C.V. 2000. *Peg1/Mest* locates distal to the currently defined imprinting region on mouse proximal chromosome 6 and identifies a new imprinting region affecting growth. *Cytogenet. Cell Genet.* **90:** 309–314.

Clark, L., Wei, M., Cattoretti, G., Mendelsohn, C., and Tycko, B. 2002. The *Tnfrh1* (*Tnfrsf23*) gene is weakly imprinted in several organs and expressed at the trophoblast-decidua interface. *BMC Genet.* **3:** 11.

Davies, H.G., Richter, R.J., Keifer, M., Broomfield, C.A., Sowalla, J., and Furlong, C.E. 1996. The effect of the human serum paraoxonase polymorphism is reversed with diazoxon, soman and sarin. *Nat. Genet.* **14:** 334–336.

Draganov, D.I., Stetson, P.L., Watson, C.E., Billecke, S.S., and La Du, B.N. 2000. Rabbit serum paraoxonase 3 (PON3) is a high-density lipoprotein-associated lactonase and protects low-density lipoprotein against oxidation. *J. Biol. Chem.* **275:** 33435–33442.

Hikichi, T., Kohda, T., Kaneko-Ishino, T., and Ishino, F. 2003. Imprinting regulation of the murine *Meg1/Grb10* and human *GRB10* genes; roles of brain-specific promoters and mouse-specific CTCF-binding sites. *Nucleic. Acids Res.* **31:** 1398–1406.

Janbon, G., Himmelreich, U., Moyrand, F., Improvisi, L., and Dromer, F. 2001. Cas1p is a membrane protein necessary for the O-acetylation of the *Cryptococcus neoformans* capsular polysaccharide. *Mol. Microbiol.* **42:** 453–467.

Kaneko-Ishino, T., Kuroiwa, Y., Miyoshi, N., Kohda, T., Suzuki, R., Yokoyama, M., Viville, S., Barton, S.C., Ishino, F., and Surani, M.A. 1995. *Peg1/Mest* imprinted gene on chromosome 6 identified by cDNA subtraction hybridization. *Nat. Genet.* **11:** 52–59.

Kobayashi, S., Vemura, T., Kohda, T., Nagai, T., Chinen, Y., Naritomi, K., Kinoshita, E.I., Ohashi, H., Imaizumi, K., Tsukahara, M., et al. 2001. No evidence of PEG1/MEST gene

mutations in Silver-Russell syndrome patients. *Am. J. Med. Genet.* **104:** 225–231.
Kosaki, K., Kosaki, R., Craigen, W.J., and Matsuo, N. 2000. Isoform-specific imprinting of the human *PEG1/MEST* gene. *Am. J. Hum. Genet.* **66:** 309–312.
Lefebvre, L., Viville, S., Barton, S.C., Ishino, F., Keverne, E.B., and Surani, M.A. 1998. Abnormal maternal behaviour and growth retardation associated with loss of the imprinted gene *Mest*. *Nat. Genet.* **20:** 163–169.
Li, T., Vu, T.H., Zeng, Z.L., Nguyen, B.T., Hayward, B.E., Bonthron, D.T., Hu, J.F., and Hoffman, A.R. 2000. Tissue-specific expression of antisense and sense transcripts at the imprinted *Gnas* locus. *Genomics* **69:** 295–304.
McNally, E.M., Ly, C.T., and Kunkel, L.M. 1998. Human ε-*sarcoglycan* is highly related to α-*sarcoglycan* (*adhalin*), the limb girdle muscular dystrophy 2D gene. *FEBS Lett.* **422:** 27–32.
Mizuno, Y., Sotomaru, Y., Katsuzawa, Y., Kono, T., Meguro, M., Oshimura, M., Kawai, J., Tomaru, Y., Kiyosawa, H., Nikaido, I., et al. 2002. *Asb4, Ata3*, and *Dcn* are novel imprinted genes identified by high-throughput screening using RIKEN cDNA microarray. *Biochem. Biophys. Res. Commun.* **290:** 1499–1505.
Nakanishi, H., Obaishi, H., Satoh, A., Wada, M., Mandai, K., Satoh, K., Nishioka, H., Matsuura, Y., Mizoguchi, A., and Takai, Y. 1997. Neurabin: A novel neural tissue-specific actin filament-binding protein involved in neurite formation. *J. Cell Biol.* **139:** 951–961.
Ng, C.J., Wadleigh, D.J., Gangopadhyay, A., Hama, S., Grijalva, V.R., Navab, M., Fogelman, A.M., and Reddy, S.T. 2001. *Paraoxonase-2* is a ubiquitously expressed protein with antioxidant properties and is capable of preventing cell-mediated oxidative modification of low-density lipoprotein. *J. Biol. Chem.* **276:** 44444–44449.
Ono, R., Kobayashi, S., Wagatsuma, H., Aisaka, K., Kohda, T., Kaneko-Ishino, T., and Ishino, F. 2001. A retrotransposon-derived gene, *PEG10*, is a novel imprinted gene located on human chromosome 7q21. *Genomics* **73:** 232–237.
Peters, J., Wroe, S.F., Wells, C.A., Miller, H.J., Bodle, D., Beechey, C.V., Williamson, C.M., and Kelsey, G. 1999. A cluster of oppositely imprinted transcripts at the *Gnas* locus in the distal imprinting region of mouse chromosome 2. *Proc. Natl. Acad. Sci.* **96:** 3830–3835.
Piras, G., El Kharroubi, A., Kozlov, S., Escalante-Alcalde, D., Hernandez, L., Copeland, N.G., Gilbert, D.J., Jenkins, N.A., and Stewart, C.L. 2000. *Zac1* (*Lot1*), a potential tumor suppressor gene, and the gene for ε-*sarcoglycan* are maternally imprinted genes: Identification by a subtractive screen of novel uniparental fibroblast lines. *Mol. Cell. Biol.* **20:** 3308–3315.
Poulter, R. and Butler, M. 1998. A retrotransposon family from the pufferfish (fugu) *Fugu rubripes*. *Gene* **215:** 241–249.
Preece, M.A., Price, S.M., Davies, V., Clough, L., Stanier, P., Trembath, R.C., and Moore, G.E. 1997. Maternal uniparental disomy 7 in Silver-Russell syndrome. *J. Med. Genet.* **34:** 6–9.
Primo-Parmo, S.L., Sorenson, R.C., Teiber, J., and La Du, B.N. 1996. The human *serum paraoxonase/arylesterase* gene (*PON1*) is one member of a multigene family. *Genomics* **33:** 498–507.
Raizis, A.M., Schmitt, F. and Jost, J.P. 1995. A bisulfite method of 5-methylcytosine mapping that minimizes template degradation. *Anal. Biochem.* **226:** 161–166.
Shih, D.M., Gu, L., Xia, Y.R., Navab, M., Li, W.F., Hama, S., Castellani, L.W., Furlong, C.E., Costa, L.G., Fogelman, A.M., et al. 1998. Mice lacking serum paraoxonase are susceptible to organophosphate toxicity and atherosclerosis. *Nature* **394:** 284–287.
Song, Z., Casolaro, V., Chen, R., Georas, S.N., Monos, D., and Ono, S.J. 1996. Polymorphic nucleotides within the human *IL-4* promoter that mediate overexpression of the gene. *J. Immunol.* **156:** 424–429.
Tsai, C., Lin, S., Ito, M., Takagi, N., Takada, S., and Ferguson-Smith, A. 2002. Genomic imprinting contributes to thyroid hormone metabolism in the mouse embryo. *Curr. Biol.* **12:** 1221.
Uejima, H., Lee, M.P., Cui, H., and Feinberg, A.P. 2000. Hot-stop PCR: A simple and general assay for linear quantitation of allele ratios. *Nat. Genet.* **25:** 375–476.
Vu, T.H. and Hoffman, A.R. 1994. Promoter-specific imprinting of the human *insulin-like growth factor-II* gene. *Nature* **371:** 714–717.
Wilson, A.G., Symons, J.A., McDowell, T.L., McDevitt, H.O., and Duff, G.W. 1997. Effects of a polymorphism in the human tumor necrosis factor α promoter on transcriptional activation. *Proc. Natl. Acad. Sci.* **94:** 3195–3199.
Zimprich, A., Grabowski, M., Asmus, F., Naumann, M., Berg, D., Bertram, M., Scheidtmann, K., Kern, P., Winkelmann, J., Muller-Myhsok, B., et al. 2001. Mutations in the gene encoding ε-*sarcoglycan* cause myoclonus-dystonia syndrome. *Nat. Genet.* **29:** 66–69.

WEB SITE REFERENCES

http://www.ebi.ac.uk/emboss/cpgplot/; CpG Island finder and plotting tool.
http://www.mgu.har.mrc.ac.uk/imprinting/imprinting.html; Mouse imprinting maps and data.

Received October 13, 2002; accepted in revised form May 12, 2003.

European Journal of Neuroscience, Vol. 17, pp. 2249–2255, 2003

Role of heme oxygenase-1 protein in the neuroprotective effects of cyclopentenone prostaglandin derivatives under oxidative stress

Takumi Satoh,[1] Megumi Baba,[1] Daisaku Nakatsuka,[2] Yasuyuki Ishikawa,[3] Hiroyuki Aburatani,[4] Kyoji Furuta,[5] Toshihisa Ishikawa,[6] Hiroshi Hatanaka,[7] Masaaki Suzuki[5] and Yasuyoshi Watanabe[2]
[1]Department of Welfare Engineering, Faculty of Engineering, Iwate University, Morioka, Iwate 020–8551, Japan
[2]Department of Physiology, Osaka City University, Graduate School of Medicine, Osaka, Japan
[3]Division of Structural Cell Biology, Nara Institute of Science and Technology, Ikoma, Nara, Japan
[4]Department of Genomic Science, Research Center for Advanced Science and Technology, The University of Tokyo, Tokyo, Japan
[5]Regeneration and Advanced Medical Science, Graduate School of Medicine, Gifu University, Gifu, Japan
[6]Department of Biomolecular Engineering, Tokyo Institute of Technology, Midori-ku, Yokohama, Japan
[7]Division of Protein Biosynthesis, Institute for Protein Research, Osaka University, Suita, Osaka, Japan

Keywords: bilirubin, cortical neurons, cyclopentenone prostaglandin, heme oxygenase-1, HT22 cells, mice, NEPP

Abstract

Previously we found that some cyclopenteone prostaglandin derivatives (PGs), referred to as neurite outgrowth-promoting PGs (NEPPs), have dual biological activities of promoting neurite outgrowth and preventing neuronal death [Satoh *et al.* (2000) *J. Neurochem.*, **75**, 1092-1102; Satoh *et al.* (2001) *J. Neurochem.*, **77**, 50-62; Satoh *et al.* (2002) In Kikuchi, H. (ed.), *Strategenic Medical Science Against Brain Attack*. Springer-Verlag, Tokyo, pp. 78-93]. To investigate possible cellular mechanisms of the neuroprotective effects, we performed oligo hybridization-based DNA array analysis with mRNA isolated from HT22, a cell line that originated from a mouse hippocampal neuron. Several transcripts up-regulated by NEPP11 were identified. Because heme oxygenase 1 (HO-1) mRNA was the most prominently induced and was earlier reported to protect neuronal and non-neuronal cells against oxidative stress, we focused on it as a possible candidate responsible for the neuroprotective effects. We found NEPP11 to induce HO-1 protein (32 kDa) in HT22 cells in both the presence and the absence of glutamate, whereas non-neuroprotective prostaglandins (PGs) Δ^{12}-PGJ_2 or PGA_2 did not. Overexpression of HO-1-green fluorescence protein (GFP) fusion protein significantly protected HT22 cells against oxidative glutamate toxicity, whereas that of GFP alone did not. Furthermore, biliverdin and bilirubin, products of HO-1 enzymatic activity on heme, protected HT22 cells from oxidative glutamate toxicity. These results, together with our previous results, suggest that NEPP11 activates the expression of HO-1 and that HO-1 produces biliverdin and bilirubin, which result in the inhibition of neuronal death induced by oxidative stress. NEPP11 is the first molecular probe reported to have a neuroprotective action through induction of HO-1 in neuronal cells.

Introduction

Neurotrophins play an essential role in the maintenance of populations of neuronal cells from development through adulthood (Barde, 1998) and thus administration of neurotrophins may be an effective treatment for disorders of neurons (McMahon & Priestly, 1995). However, being proteins, neurotrophins are not ideal drug candidates owing to the low permeability of the blood–brain barrier to them. Therefore, much effort has been made in the search for non-peptidyl low-molecular-weight compounds (Saragovi & Gehring, 2000). Recently, we accumulated several lines of evidence showing that neurite outgrowth-promoting prostaglandins 11 (NEPP11) has neurotrophin-like, Trk-independent actions on central nervous system (CNS) neurons (Furuta *et al.*, 2000; T. Satoh *et al.*, 2000a, 2001). NEPP11 (a Δ^7-PG A_1 methyl ester derivative) was originally designed on the basis of the chemical structure of Δ^{12}-PGJ_2 (Fukushima, 1992; Suzuki *et al.*, 1997, 1998; Furuta *et al.*, 2000). NEPP11 is a novel type of neuroprotective compound characterized by its dual biological activities of promoting neurite outgrowth and preventing neuronal death (T. Satoh *et al.*, 2000a, b, 2001). Generally, the cyclopentenone-structured PGAs and PGJs exhibit antitumour activities both *in vivo* and *in vitro* (Honn *et al.*, 1981; Fukushima, 1992; Suzuki *et al.*, 1997, 1998). They accumulate in the nuclear fraction, where they bind to nuclear proteins (Narumiya *et al.*, 1987; Parker, 1995) and thereby modulate the expression of various genes (Holbrook *et al.*, 1992; Gorospe *et al.*, 1996; Ishikawa *et al.*, 1998; Tanikawa *et al.*, 1998). Transcriptional activation is required for the biological actions by the cyclopentenone-structured PGs (Fukushima, 1992). Thus, identification of the gene(s) responsible for their biological effects is critical to understand their intracellular mechanisms. Previous results suggest that induction of immunoglobulin heavy chain binding protein/glucose-regulated protein 78 plays a role in the promotion of neurite outgrowth by NEPPs (T. Satoh *et al.*, 2000a). During the comparison of biological activities among various PG derivatives, we noted that the intracellular mechanism involved in the neuroprotection was different from that involved in the promotion of neurite outgrowth (T. Satoh *et al.*, 2001).

Correspondence: Dr T. Satoh, as above.
E-mail: tsatoh@iwate-u.ac.jp

Received 18 December 2002, revised 31 March 2003, accepted 4 April 2003

doi:10.1046/j.1460-9568.2003.02688.x

In the present study, a DNA microarray analysis was performed to identify the gene responsible for the neuroprotective effect mediated by NEPP11. We found that the induction of heme oxygenase 1 (HO-1) protein plays a role in this neuroprotection. Finally, we propose that the differential regulations of HO-1/HO-2 activities comprise a transient- and sustained-phase cellular defence mechanism and co-operatively contribute to the maintenance of neuronal survival under oxidative conditions.

Materials and methods

Materials

PGA_2, Δ^{12}-PGJ_2 (Cayman Chemical, Ann Arbor, MI, USA), 3-(4,5-dimethylthiazol-2-yl)-2,5-diphenyl tetrazolium bromide (MTT; Research Organics, Cleveland, OH, USA), polyclonal antibody against rat HO-1 (SPA895, Stressgen, Victoria, Canada), biotinylated anti-rabbit IgG secondary antibody (Vector Laboratories, Burlingame, CA, USA), Cy™3 (Cy3)-conjugated streptavidin (Jackson Immuno Research Laboratories, West Grove, PA, USA), peroxidase-conjugated anti-rabbit IgG antibody (Biorad, Hercules, CA, USA), biliverdin, bilirubin and Hoechst 33,258 (Sigma, St. Louis, MO, USA) were used in this study. NEPPs were synthesized as reported previously (Furuta *et al.*, 2000).

HT22 cell culture

HT22 cells were cultured as described (T. Satoh *et al.*, 2000c). To evaluate cell survival of HT22 cells, we performed MTT assay according to a modification (Kubo *et al.*, 1995) of the original procedure (Mosmann, 1983).

RT-PCR analysis

For reverse transcription-polymerase chain reaction (RT-PCR) analysis of HO-1 mRNA, total RNA of HT22 cells was obtained at 0.5, 1.0, 2.0, 5.0 and 8.0 h after glutamate treatment by use of TRIZOL Reagent (Invitrogen Corp., Carlsbad, CA, USA). Total RNA 1 μg was exposed to MMLV reverse transcriptase (50 U) in the presence of RNasin (20 U), random hexamers (2.5 μM), dNTPs and the supplied reverse transcription buffer. The reaction (20 μL) was allowed to continue for 15 min at 42 °C. A 10-μL aliquot of this mixture was then subjected to PCR conducted with HO-1 (5′-ACT TTC AGA AGG GTC AGG TGT CC-3′ and 5′-TTG AGC AGG AAG GCG GTC TTA G-3′) or GAPDH (5′-ATG CCA GTG GC TTC CCG TTC AGC-3′ and 5′-ACC CCT TCA TTG ACC TCA ACT-3′) primers (5 μM each). At the completion of PCR, 10 μL of PCR products was mixed with 2 μL of loading buffer and electrophoresed in 1.5% agarose gel in the presence of 0.5 μg/mL of ethidium bromide. The amplified DNA fragments (523 and 504 bp for HO-1 and GAPDH, respectively) were visualized with a UV transilluminator.

DNA microarray analysis

Total RNA was obtained after a 6-h treatment of HT22 cells with glutamate or vehicle in the presence or absence of NEPP11 (1 μM) and subjected to DNA microarray analysis as described previously (Ishii *et al.*, 2000) by use of a DNA microarray plate (Genechip, Affymetrix, Santa Clara, CA, USA).

Western blot analysis

HT22 cells were lysed in cell lysis buffer after 24 h of glutamate treatment, as described previously (T. Satoh *et al.*, 2000c). The protein signals were detected with anti-rat HO-1 polyclonal antibody and enhanced by chemiluminesence (ECL™ Western blotting; Amersham Pharmacia Biotech., Buckinghamshire, UK).

Immunofluorescence analysis of HO-1

HT22 cells were fixed after 24 h of incubation with or without NEPP11 (1 μM). The signals originated from polyclonal antibody against rat HO-1 were enhanced by biotinylated anti-rabbit IgG secondary antibody followed by detection with Cy™3 (Cy3)-conjugated streptavidin as described previously (T. Satoh *et al.*, 2000a).

DNA construction and transfection

PCR was performed using rat HO-1 primers (5′-CTC AGA TCT ATG GAG CGC CCA CAG C-3′ and 5′-TCG AAG CTT CAT GGC ATA AAT TCC CAC TG-3′) and pCRHO-1 as a templete (Shibahara *et al.*, 1985), and then the PCR product was digested with *Bgl*II and *Hin*dIII and cloned in pEGFPN1 and pEGFPC1 (Clontech Laboratories Inc., Palo Alto, CA, USA). These resulting vectors, pHON1 and pHOC1, can express rat HO-1 protein fused in-frame with the N- and C-terminal portion of EGFP, respectively. DNA transfection was performed by a particle bombardment method using the PDS-1000He particle delivery system (Bio-Rad) as described previously (H. Satoh *et al.*, 2000) according to the manufacturer's instructions. Recently this method was reported to allow highly efficent DNA transfection of primary neurons (McAllister, 2000).

Results

NEPP11 had a potent protective effect on HT22 cells (Satoh *et al.*, 2001). A high concentration of glutamate in the culture medium induced neuronal death through oxidative stress 10 h after the exposure of glutamate as described previously (Schubert *et al.*, 1992; Davis & Maher, 1994; Tan *et al.*, 1998). The presence of NEPP11 (1.0 μM) almost completely protected HT22 cells against this toxicity (Satoh *et al.*, 2001).

To identify the gene responsible for the neuroprotective effect of NEPP11, we performed a DNA microarray analysis. Total RNA was isolated from control HT22 cells or the cells treated with NEPP11 (1.0 μM) for 6 h in the presence or the absence of glutamate (5 mM) and was subjected to reverse transcription and oligo hybridization-based DNA array analysis. Three genes showed significantly increased expression (sort score >1.5) in response to NEPP11 both in the presence and in the absence of glutamate. The sort score is used in DNA microarray analysis as a parameter to indicate data reliance of gene induction. These three genes encode stress proteins, HO-1, α-B-crystallin and tissue inhibitor of metalloproteinase-3 (TIMP-3). The fold increase of induction/sort score of HO-1, α-B-crystallin and TIMP3 was 4.1/2.65, 4.7/3.16 and 4.6/2.65, respectively; and in the presence of glutamate, 5.1/4.22, 3.3/1.51 and 3.9/1.9, respectively.

In this study, although the expression of α-B-crystallin and TIMP-3 were elevated by NEPP11, we focused on HO-1 for the following reasons: (1) cerebellar granule neurons from HO-1-transgenic mice are resistant to oxidative stress (Chen *et al.*, 2000), (2) gene transfer of α-B-crystallin did not protect fibroblasts from oxidative stress (Mehlen *et al.*, 1996) and (3) gene transfer of TIMP-3 enhanced cell death (Bian *et al.*, 1996). At first, the data from the DNA microarray analysis were confirmed by a RT-PCR experiment (Fig. 1A). Total RNA was extracted at various times after the addition of NEPP11 and subjected to reverse transcription by use of random primers and to PCR with primers for HO-1 and GAPDH. Although the levels of GAPDH mRNA was constant during the experiment, HO-1 mRNA was present at a very low level in control cells and increased between 0.5 and 2.0 h after the addition of NEPP11, suggesting that HO-1 mRNA was up-regulated by NEPP11. Next, using Western blotting, we examined the induction of HO-1 protein by various cyclopentenone PGs (Fig. 1B). Neuroprotective NEPP6 and NEPP11 increased the expression of

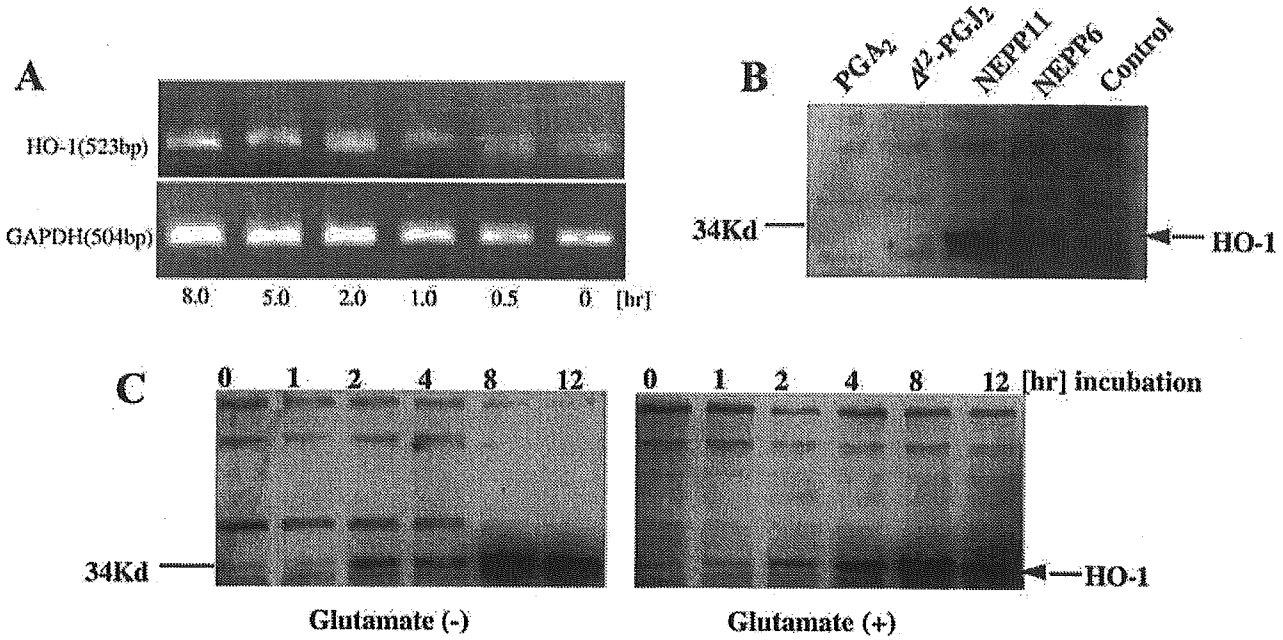

FIG. 1. (A) Time-dependent expression of HO-1 mRNA induced by NEPP11. HT22 cells were incubated for 0, 0.5, 1.0, 2.0, 5.0 or 8.0 h with NEPP11, and then total RNA was extracted and subjected to reverse transcription and to PCR with HO-1 or GAPDH primers. (B) Induction of HO-1 protein (32 kDa) by 1 μM NEPP6, 1 μM NEPP11, 2 μM PGA_2 or 2 μM Δ^{12}-PGJ_2. HT22 cells were incubated with various cyclopentenone PGs for 24 h, and then their lysates were subjected to Western blotting. (C) Time-dependent induction of HO-1 protein by 1 μM NEPP11. HT22 cells were cultured for various periods of time with 1 μM NEPP11 in the presence (right) or absence (left) of glutamate (5 mM), and then their lysates were prepared and subjected to Western blotting.

HO-1. In contrast, non-neuroprotective Δ^{12}-PGJ_2 and PGA_2 did not induce the protein. Time-dependent induction of HO-1 protein by 1 μM NEPP11 was examined in both the presence and the absence of 5 mM glutamate (Fig. 1C). The level of HO-1 protein increased after 2 h of incubation and reached its maximum at 8 h (Fig. 1C, left). The presence of glutamate did not make much difference (Fig. 1C, right). The induction of HO-1 was also confirmed by immunofluorescence (Fig. 2A and B). In this experiment, the average fluorescence intensity (arbitrary unit) in each designated square was obtained to provide quantitative comparison between control and NEPP11-treated cells. The NEPP11-treatd cells had much higher intensity [177.6 ± 22.8, mean ± SD ($n = 10$)] than did the control cells [83.5 ± 5.6 ($n = 10$)], indicating that NEPP11 effectively induced HO-1 protein in HT22 cells.

To provide evidence for the neuroprotective effects of HO-1 protein, we performed a gene transfer experiment by use of particle bombardment (Fig. 3). HO-1 protein fused in-frame to the C-terminal portion of GFP, termed GFP–HO-1, or GFP protein alone, could be expressed under the regulation of the CMV promoter. The transfection efficiency was $28.3 \pm 7.3\%$ of all cells (mean ± SD, $n = 6$). The expression patterns of GFP and GFP–HO-1 were quite different (Fig. 3A and B). GFP was sparsely expressed throughout the cells (Fig. 3A); in contrast, GFP–HO-1 was expressed in a particle-like fashion mainly in the cytoplasm (Fig. 3B). This pattern was identical to that of HO-1 protein fused in-frame to the N-terminal portion of GFP (HO-1–GFP)-expressed cells (data not shown). The cells transfected with GFP alone shrank 24 h after the addition of glutamate (Fig. 3C), whereas those transfected with GFP–HO-1 did not shrink after the additon of glutamate (Fig. 3D). We did not utilize DNA staining with propidium iodide or Hochest 33,258 for detection of cell death because non-transfected DNA was tightly attached to the cell surface, which would interfere with the measurement. Thus, we assessed death by cell shrinkage (<20 μm), which occurrs in neuronal death. The presence of glutamate for 24 h increased the number of shrunken cells transfected with GFP [$87.5 \pm 14.4\%$ of transfected cells ($n = 4$)]. In contrast, the cells transfected with GFP–HO-1 were much less shrunken [$6.25\% \pm 3.5\%$ ($n = 4$)] in the presence of glutamate. Similar results were obtained with the use of HO-1–GFP. These results show that the cells survived effectively when HO-1 protein was induced.

Is the enzymatic activity of HO-1 required for the neuroprotective effects? As biliverdin and bilirubin are products of HO-1 catalysis, we examined their effects on HT22 cells (Fig. 4). Both biliverdin and bilirubin significantly protected HT22 cells against oxidative glutamate toxicity, suggesting that the enzymatic activity of HO-1 plays some role in the inhibition of death of HT22 cells.

Discussion

HO cleaves heme molecules at the α-meso carbon bridge and produces the open tetrapyrrole biliverdin. This enzyme family comprises three isozymes, HO-1, HO-2 and HO-3. HO-1 and HO-2 have a different gene expression pattern (Maines, 1997). In contrast to the constitutive isoform HO-2, HO-1 is the heat shock/stress-inducible cognate of the heat shock protein 32 and is induced by its substrate heme and numerous stress stimuli such as UV light, heavy metals, lipopolysaccharide and hyperoxia (Shibahara, 1994; Maines, 1997). In the brain, HO-2 protein is abundantly expressed in neuronal populations, whereas HO-1 is expressed to a far lower level, and its level is markedly increased in glial cells in response to oxidative stress (Ewing & Maines, 1991). The activity of HO-2 is regulated by phosphorylation, and that of HO-1 at the transcriptional level (Shibahara, 1994; Maines, 1997; Dore *et al.*, 1999). Dore *et al.* (1999) reported that HO-2

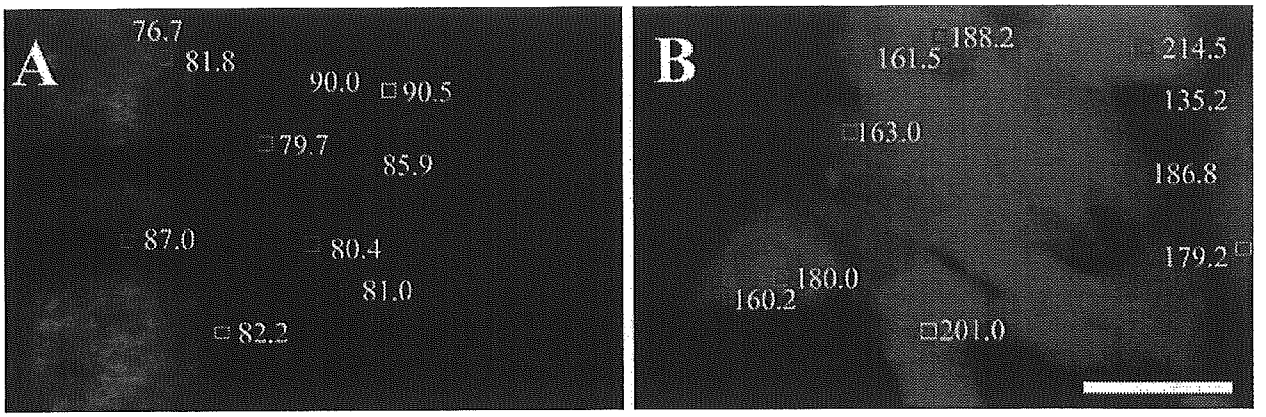

FIG. 2. Immunofluorescence analysis of HO-1 induction in HT22 cells. HT22 cells were treated with vehicle (A) or with 1 μM NEPP11 (B) for 24 h, and then the cells were fixed and stained with anti-(HO-1) antibody. The values in the photographs are average fluorescence intensity (arbitrary units) in the designated squares. Scale bar in B represents 20 μm.

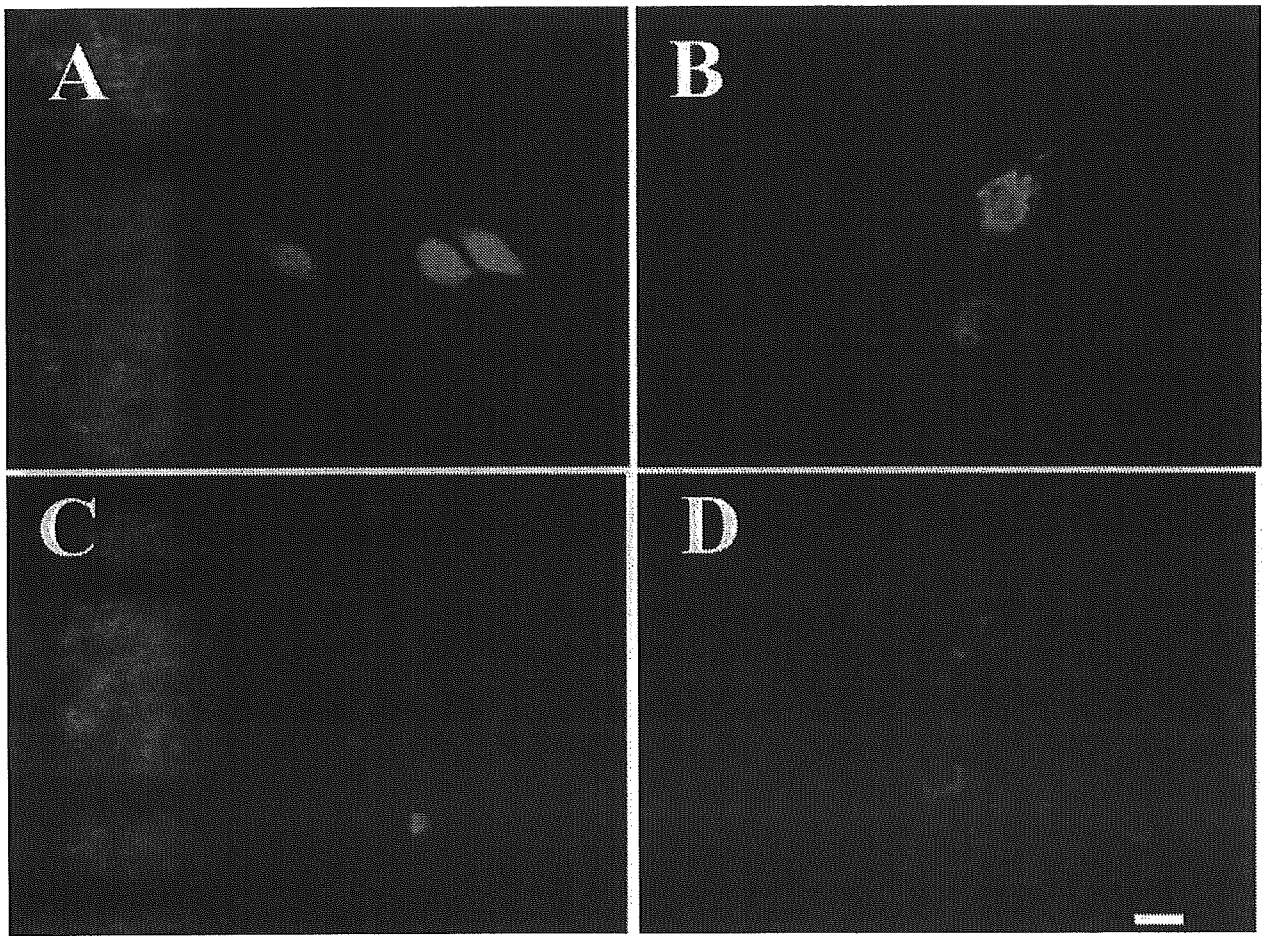

FIG. 3. Protection of HT22 cells against oxidative glutamate toxicity by gene transfer of HO-1. HT22 cell transfected with pEGFPC1 (GFP only, A and C) or pHOC1 (GFP–HO-1, B and D) were incubated for 12 h. Then, glutamate (C and D) or vehicle (A and B) was added; and 24 h later the cells were fixed and observed under a fluorescence microscope. Scale bar in D represents 20 μm.

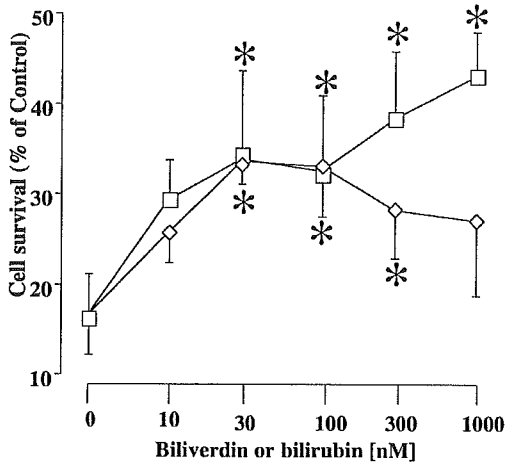

FIG. 4. Effect of biliverdin and bilirubin on the oxidative glutamate toxicity of HT22 cells. HT22 cells were treated with various concentrations of biliverdin or bilirubin in addition to 5 mM glutamate and were then lysed for the MTT assay at 24 h. Open squares, biliverdin; diamonds, bilirubin. The values, which represent the percentage of the control MTT activity, are means + SD ($n = 4$). Significance of the difference in value in the presence of biliverdin or bilirubin vs. the control value (in the absence of these compounds) was determined by ANOVA ($^*P < 0.05$).

catalytic activity was enhanced by phosphorylation and showed that C-kinase, activated by phorbol,12-myristate,13-acetate (PMA), phosphorylated HO-2, resulting in increased activity and that it protects neurons against oxidative stress through enhanced production of biliverdin and bilirubin. In contrast, NEPP11, by inducing HO-1 protein in neurons, caused the cells to produce biliverdin and bilirubin, both of which seem to be responsible for the inhibition of cell death induced by oxidative stress.

We propose an intracellular mechanism for the neuroprotective effect of NEPP11 in Fig. 5. NEPP11 covalently binds to some nuclear protein, and induces HO-1 protein (Narumiya *et al.*, 1987; Parker, 1995; Satoh *et al.*, 2001). The induction of HO-1 is an event responsible for the inhibition of neuronal death by NEPP11 based on the following results. (1) Neuroprotective NEPP6 and NEPP11 induced HO-1 protein in neuronal cells both in the presence and in the absence of glutamate (Fig. 1B); (2) neither non-neuroprotective PG (PGA_2 nor Δ^{12}-PGJ_2) protected the cells or induced HO-1 protein (Fig. 1C); (3) gene transfer of HO-1 protected HT22 cells against oxidative stress (Fig. 3) and (4) biliverdin and bilirubin, products of HO, actively protected HT22 cells against oxidative stress (Fig. 4). NEPP11 binds to cellular protein(s) and activates transcription of HO-1 to protect neurons presumably through enhanced production of biliverdin and bilirubin (Fig. 5). In contrast to a sustained phase of regulation of HO activity derived from HO-1 gene transcription, neurons can also have a transient phase of regulation of HO activity derived from HO-2 protein phosphorylation. Neurons exposed to acute oxidative stress activate HO-2 to resist this stress via phosphorylation of HO-2, whereas those exposed to chronic oxidative stress activate HO-1 through transcription. Regulations of 'heme-pool' by HO-1 and HO-2 have distinct roles in neuronal survival and are highly critical for the resistance to oxidative stress. HO-2 is rapidly activated by phosphorylation, but its activated state is not sustained. In contrast, the HO-1 level is slowly increased by transcription, and is sustained. We consider that these differential regulations of HO activities may co-operatively contribute to the maintenance of neuronal survival under oxidative conditions. Strong therapeutic implications of HO-1 induction in neuronal diseases associated with oxidative stress were provided by the findings that HO-1-deficient mice were strongly susceptible to the deleterious effects of endotoxin or hypoxia (Poss & Tonegawa, 1997; Yet *et al.*, 1999).

Bilirubin, the end-product of heme catabolism in mammals, is generally regarded as a potentially cytotoxic, lipid-soluble waste product that needs to be excreted. However, recent studies suggest that the resultant accumulation of biliverdin and bilirubin might afford a neuroprotective mechanism against oxidative stress. In the present study, bilirubin as well as biliverdin protected HT22 cells at concentrations in the nanomolar range (Fig. 4). Consistent with this finding, Dore *et al.* (1999) also reported that these compounds protected primary cortical neurons against hydrogen peroxide toxicity at similar concentrations. These pharmacological studies suggest that low concentrations (below micromolar levels) of biliverdin and bilirubin might have a neuronal survival effect in the brain, whereas higher concentrations (above micromolar levels) of blirubin were shown to induce neuronal death (Grojean *et al.*, 2000). What is the mechanism of the neuroprotective effects afforded by these endogenous compounds? Several possibilities were postulated by previous investigators. One is the scavenging of free radicals (Stocker *et al.*, 1987), and another is inhibition of protein phosphorylation (Hansen *et al.*, 1997). Because

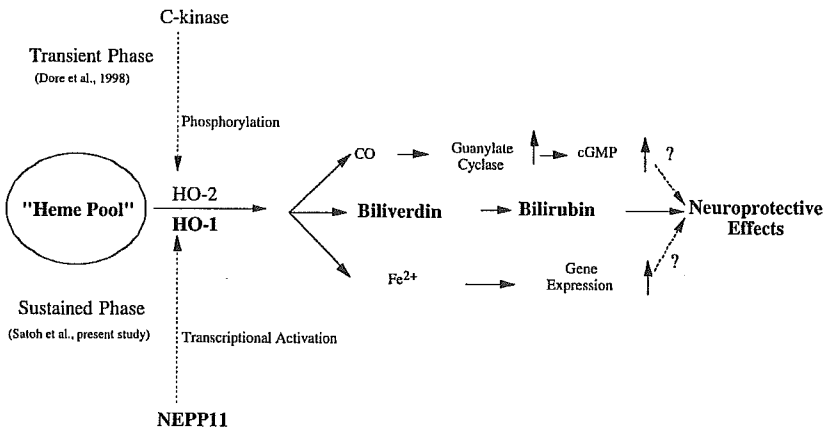

FIG. 5. Proposed mechanism for neuronal survival-promoting effect of NEPP11.

the generation of free radicals (Tan *et al.*, 1998) and protein phosphorylation, for example by ERK1/2 (T. Satoh *et al.*, 2000c; Stanciu *et al.*, 2000), plays a central role in the death of HT22 cells by oxidative glutamate toxicity, inhibition of these events may contribute to inhibition of cell death. The problem is that a high concentration (above micromolar level) of bilirubin is required to produce these actions. Thus, some other unknown mechanism might be responsible for the inhibition of cell death by bilirubin and biliverdin. If not, then several neuroprotective events triggered by induction of HO-1 other than production of biliverdin and bilirubin might be possible. For example, CO is suspected to be a signalling molecule to modulate guanylate cyclase activity and to produce cGMP (Maines, 1997; Zakhary *et al.*, 1997), which reportedly protects primary neurons (Keller *et al.*, 1998).

The biological significance of HO-1 induction has remained a matter of debate. The most essential question is whether HO-1 protects or kills neurons. Schipper (2000) suggested that HO-1 overexpression contributes to pathological iron deposition and mitochondrial damage in ageing-related neurodegenerative disorders. Metalloporphyrins, inhibitors of HO, protected astroglial cells against hydrogen peroxide toxicity (Dwyer *et al.*, 1998). These results suggest that the induction of HO-1 is cytotoxic. However, *in vitro* studies suggest neuroprotective effects of HO-1. Culture experiments to examine the role of HO-1 in neuronal survival were conducted by two groups. One (Le *et al.*, 1999) reported the use of antisense nucleotides; and the other (Chen *et al.*, 2000) reported the use of primary neurons from mice overexpressing HO-1. HO-1 was induced in response to a variety of oxidative stresses including β-amyloid peptides and hydrogen peroxide in neuronal cells; and pretreatment with HO-1 antisense nucleotides enhanced the cytotoxicity, whereas hemin, an HO-1 inducer, decreased the toxicity (Le *et al.*, 1999). Cerebellar granule neurons from mice overexpressing HO-1 resisted glutamate toxicity by decreasing the levels of free radicals (Chen *et al.*, 2000). In addition, CNS neurons of HO-1 transgenic mice were resistant to permanent brain ischaemia (Panahian *et al.*, 1999). These results suggest that HO-1 protein is induced under oxidative conditions and that the HO-1 protein protects neurons against oxidative stress. In view of our results and those of others, it is possible that the enhanced expression of HO-1 in the neurodegenerative areas is not a cause of cell damage but a result of cell defence against oxidative stress.

Natural cyclopentenone PGs (Δ^{12}-PGJ_2 and *15-deoxy*-$\Delta^{12,14}$-PGJ_2) were shown to induce HO-1 protein in non-neuronal cells (Koizumi *et al.*, 1995; Negishi *et al.*, 1995; Clay *et al.*, 2001). Negishi *et al.* (1995) reported that Δ^{12}-PGJ_2 potently induced HO-1 in leukaemia cells through phosphorylation of nuclear protein. The induction of HO-1 protein may contribute to the anti-tumour effects of Δ^{12}-PGJ_2 because adenoviral gene transfer of HO-1 reportedly arrested the cell cycle of, and induced apoptosisin, vascular smooth muscle cells proliferating in response to serum (Liu *et al.*, 2002). In contrast to an apoptosis-inducing effect on proliferating cells, induced HO-1 seems to inhibit cell death in post-mitotic CNS neurons. For example, administration of HO-1 cDNA via viral vectors decreased the volume of infarct induced in the brain by permanent ischaemia, suggesting that HO-1 induction is neuroprotective (Panahian *et al.*, 1999). NEPP11 potently induced HO-1 in cortical neurons (data not shown) as well as HT22 cells and protected them at similar concentrations (Satoh *et al.*, 2001). Furthermore, NEPP11 also reduced the volume of infarct induced by permanent ischaemia (Satoh *et al.*, 2001). In this context, NEPP11 is a novel molecular probe both *in vivo* and *in vitro* for the investigation of neuroprotective HO-1 inducer against oxidative stress. In contrast, non-neuroprotective cyclopentenone PGs such as PGA_1, PGA_2, Δ^{12}-PGJ_2 and *15-deoxy*-$\Delta^{12,14}$-PGJ_2 neither protected HT22 cells (Satoh *et al.*, 2001) nor induced HO-1 protein in them (Fig. 1). The differential response to Δ^{12}-PGJ_2 between neuronal and non-neuronal cells remains to be analysed, but it might be dependent on the cell types used. Alternatively, the toxicity of Δ^{12}-PGJ_2 toward neurons might mask the neuroprotective effects of this PG.

Acknowledgements

This work was supported in part by the Research for the Future Program (RFTF) JSPS-RFTF 98L00201 of the Japan Society for the Promotion of Science (JSPS) and by Special Coordination Funds for Promoting Science and Technology from the Science and Technology Agency (Japan). We thank Dr Larry D. Frye for editorial help with the manuscript.

Abbreviations

GFP, green fluorescence protein ; HO, heme oxygenase; NEPP11, neurite outgrowth-promoting prostaglandins 11; PG, prostaglandin.

References

Barde, Y.A. (1998) Biological roles of neurotrophins. In Hefti, F. (Ed.), *Neurotrophic Factors.* Springer, Berlin, pp. 1–31.

Bian, J., Wang, Y., Smith, M.R., Kim, H., Jacobs, C., Jackman, J., Kung, H.F., Colburn, N.H. & Sun, Y. (1996) Suppression of in vivo tumor growth and induction of suspension cell death by tissue inhibitor of metalloproteinases (TIMP)-3. *Carcinogenesis*, **17**, 1805–1811.

Chen, K., Gunter, K. & Maines, M.D. (2000) Neurons overexpressing heme oxygenase-1 resist oxidative stress-mediated cell death. *J. Neurochem.*, **75**, 304–313.

Clay, C.E., Atsumi, G., High, K.P. & Chilton, F.H. (2001) Early de novo gene expression is required for *15-deoxy*-$\Delta^{12,14}$-prostaglandin J_2-induced apoptosis in breast cancer cells. *J. Biol. Chem.*, **276**, 47131–47135.

Davis, J.B. & Maher, P. (1994) Protein kinase C activation inhibits glutamate-induced cytotoxicity in a neuronal cell line. *Brain Res.*, **652**, 169–173.

Dore, S., Takahashi, M., Ferris, C.D., Hester, L.D., Guastella, D. & Snyder, S.H. (1999) Birilubin, formed by activation of heme oxygenase-2, protects neurons against oxidative stress injury. *Proc. Natl Acad. Sci. USA*, **96**, 2445–3450.

Dwyer, B.E., Lu, S.Y., Laitinen, J.T. & Nishimura, R.N. (1998) Protective properties of tin- and manganese-centered porphyrins against hydrogen peroxide-mediated injury in rat astroglial cells. *J. Neurochem.*, **71**, 2497–2504.

Ewing, J.F. & Maines, M.D. (1991) Rapid induction of heme oxygenase-1 mRNA and protein by hyperthermia in rat brain: heme oxygenase-2 is not a heat shock protein. *Proc. Natl Acad. Sci. USA*, **88**, 5364–5368.

Fukushima, M. (1992) Biological activities and mechanism of action of PGJ_2 and related compounds: an update. *Prostagl. Leukotri. Essen. Fatty Acids*, **47**, 1–12.

Furuta, K., Tomokiyo, K., Satoh, T., Watanabe, Y. & Suzuki, M. (2000) Designed prostaglandins with neurotrophic activities. *Chembiochem.*, **1**, 283–286.

Gorospe, M., Wang, X., Guyton, K.Z. & Holbrook, N.J. (1996) Protective role of $p21^{Waf1/Cip1}$ against prostaglandin A_2-mediated apoptosis of human colorectal carcinoma cells. *Mol. Cell. Biol.*, **16**, 6654–6660.

Grojean, S., Koziel, V., Vert, P. & Daval, J.L. (2000) Bilirubin induces apoptosis via activation of NMDA receptors in developing rat brain. *Exp. Neurol.*, **166**, 334–341.

Hansen, T.W., Mathiesen, S.B. & Walaas, S.I. (1997) Modulation of the effect of bilirubin on protein phosphorylation by lysine-containing peptides. *Pediatr. Res.*, **42**, 615–617.

Holbrook, N.J., Carlson, S.G., Choi, A.M.K. & Fargnoli, J. (1992) Induction of HSP70 gene expression by antiproliferative prostaglandin PGA_2: a growth-dependent response mediated by activation of heat shock transcription factor. *Mol. Cell. Biol.*, **12**, 1528–1538.

Honn, K.V., Bockman, R.S. & Marnett, L.J. (1981) Prostaglandins and cancer: a review of tumor initiation through tumor metastasis. *Prostaglandins*, **21**, 833–864.

Ishii, M., Hashimoto, S., Tsutsumi, S., Wada, Y., Matsushima, K., Kodama, T. & Aburatani, H. (2000) Direct comparison of Genechip and SAGE on the quantitative accuracy in transcript profiling analysis. *Genomics*, **68**, 136–143.

Ishikawa, T., Akimaru, K., Nakanishi, M., Tomokiyo, K., Furuta, K., Suzuki, M. & Noyori, R. (1998) Anticancer prostaglandin-induced cell cycle arrest and its modulation by GS-X pump inhibitor. *Biochem. J.*, **336**, 569–576.

Keller, J.N., Hanni, K.B., Mattson, M.P. & Markesbery, W.R. (1998) Cyclic nucleotides attenuate lipid peroxidation-mediated neuron toxicity. *Neuroreport*, **16**, 3731–3734.

Koizumi, T., Odani, N., Okuyama, T., Ichikawa, A. & Negishi, M. (1995) Identification of a cis-regulatory element for delta 12-prostaglandin J_1-induced expression of the rat heme oxygenase gene. *J. Biol. Chem.*, **270**, 21779–21784.

Kubo, T., Nonomura, T., Enokido, Y. & Hatanaka, H. (1995) Brain-derived neurotrophic factor (BDNF) can prevent apoptosis of rat cerebellar granule neurons in culture. *Dev. Brain Res.*, **85**, 249–258.

Le, W., Xie, W. & Appel, S.H. (1999) Protective role of heme oxygenase-1 in oxidative stress-induced neuronal injury. *J. Neurosci. Res.*, **56**, 652–658.

Liu, X.M., Chapman, G.B., Wang, H. & Durante, W. (2002) Adenovirus-mediated heme oxygenase-1 gene expression stimulates apoptosis in vascular smooth muscle cells. *Circulation*, **105**, 79–84.

Maines, M.D. (1997) The heme oxygenase system: a regulation of second messenger gases. *Annu. Rev. Pharmacol. Toxicol.*, **37**, 517–554.

McAllister, A.K. (2000) Biolistic transfection of neurons. Sci. STKE PL1.

McMahon, S.B. & Priestly, J.V. (1995) Peripheral neuropathies and neurotrophic factors: animal model and clinical perspectives. *Curr. Opin. Neurbiol.*, **5**, 614–616.

Mehlen, P., Kretz-Remy, C., Preville, X. & Arrigo, A.P. (1996) Human hsp27, *Drosophila* hsp27 and human alphaB-crystallin expression-mediated increase in glutathione is essential for the protective activity of these proteins against TNFalpha-induced cell death. *EMBO J.*, **15**, 2695–2706.

Mosmann, T. (1983) Rapid colorimetric assay for cellular growth and survival: application to proliferation and cytotoxic assay. *J. Immunol. Methods*, **65**, 55–63.

Narumiya, S., Ohno, K., Fukushima, M. & Fujiwara, M. (1987) Site and mechanism of growth inhibition by prostaglandins. III. Distribution and binding of prostaglandin A_2 and Δ^{12}-prostaglandin J_2 in nuclei. *J. Pharmacol. Exp. Therap.*, **242**, 306–311.

Negishi, M., Odani, N., Koizumi, T., Takahashi, S. & Ichikawa, A. (1995) Involvement of protein kinase in delta12-prostaglandin J2-induced expression of rat heme oxygenase-1 gene. *FEBS Lett.*, **372**, 279–282.

Panahian, N., Yoshihara, M. & Maines, M.D. (1999) Overexpression of heme oxygenase-1 is neuroprotective in a model of permanent middle cerebral artery occlusion in transgenic mice. *J. Neurochem.*, **72**, 1187–1203.

Parker, J. (1995) Prostaglandin A_2 protein interactions and inhibition of cellular proliferation. *Prostaglandins*, **50**, 359–375.

Poss, K.D. & Tonegawa, S. (1997) Reduced stress defense in heme oxygenase 1-deficient cells. *Proc. Natl Acad. Sci. USA*, **94**, 10925–10930.

Saragovi, H.U. & Gehring, K. (2000) Development of pharmacological agents for targeting neurotrophins and their receptors. *Trends Phamarcol. Sci.*, **21**, 93–98.

Satoh, H., Matsuda, H., Kawamura, T., Isogai, M., Yoshikawa, N. & Takahashi, T. (2000) Intracellular distribution, cell-to-cell trafficking and tubule-inducing activity of the 50 kDa movement protein of *Apple chlorotic leaf spot virus* fused to green fluorescent protein. *J. Gen. Virol.*, **81**, 2085–2093.

Satoh, T., Furuta, K., Suzuki, M. & Watanabe, Y. (2002) Neurite outgrowth-promoting prostaglandins that act as neuroprotective agents against brain ischemia and may enhance recovery of higher neuronal functions. In Kikuchi, H. (Ed.), *Strategenic Medical Science Against Brain Attack.* Springer-Verlag, Tokyo, pp. 78–93.

Satoh, T., Furuta, K., Tomokiyo, K., Nakatsuka, D., Miura, M., Hatanaka, H., Ikuta, K., Suzuki, M. & Watanabe, Y. (2000a) Facilitatory roles of novel compounds designed from cyclopentenone prostaglandins on the neurite outgrowth-promoting activities of NGF. *J. Neurochem.*, **75**, 1092–1102.

Satoh, T., Furuta, K., Tomokiyo, K., Namura, S., Nakatsuka, D., Sugie, Y., Ishikawa, Y., Hatanaka, H., Suzuki, M. & Watanabe, Y. (2001) Neurotrophic actions of novel compounds designed from cyclopentenone prostaglandins. *J. Neurochem.*, **77**, 50–62.

Satoh, T., Furuta, K., Tomokiyo, K., Suzuki, M. & Watanabe, Y. (2000b) Designed cyclopentenone prostaglandin derivatives as neurite outgrowth-promoting compounds for CAD cells, a rat catecholaminergic neuronal cell line of the central nervous system. *Neurosci. Lett.*, **291**, 167–170.

Satoh, T., Nakatauka, D., Watanbabe, Y., Nagata, N., Kikichi, H. & Namura, S. (2000c) Neuroprotection by MEK/ERK kinase inhibition against oxidative stress in a mouse neuronal cell line and rat primary cultured neurons. *Neurosci. Lett.*, **288**, 163–166.

Schipper, H.M. (2000) Heme oxygenase-1: role in brain aging and neurodegeneration. *Exp. Gerentol.*, **35**, 821–830.

Schubert, D., Kimura, H. & Maher, P. (1992) Growth factors and vitamin E modify neuronal glutamate toxicity. *Proc. Natl Acad. Sci. USA*, **89**, 8264–8267.

Shibahara, S. (1994) Heme oxygenase-regulation and physiological implication in heme metabolism. In Fujita, H. (Ed.), *Regulation of Heme Protein Synthesis.* AlphaMed. Press, Dyton, pp. 103–116.

Shibahara, S., Muller, R., Taguchi, H. & Yoshida, T. (1985) Cloning and expression of cDNA for rat heme oxygenase. *Proc. Natl Acad. Sci. USA*, **82**, 7865–7869.

Stanciu, M., Wang, Y., Kentor, R., Burke, N., Watkins, S., Kress, G., Reynolds, I., Klann, E., Angiolieri, M.R., Johnson, J.W. & DeFranco, D.B. (2000) Persistent activation of ERK contributes to glutamate-induced oxidative toxicity in a neuronal cell line and primary cortical neuron cultures. *J. Biol. Chem.*, **275**, 12200–12206.

Stocker, R., Yamamoto, Y., McDonagh, A.F., Glazer, A.N. & Ames, B.N. (1987) Bilirubin is an antioxidant of possible physiological importance. *Science*, **235**, 1043–10436.

Suzuki, M., Kiho, T., Tomokiyo, K., Furuta, K., Fukushima, S., Takeuchi, Y., Nakanishi, M. & Noyori, R. (1998) Rational design of antitumor prostaglandins with high biological stability. *J. Med. Chem.*, **41**, 3084–3090.

Suzuki, M., Mori, M., Niwa, T., Hirata, R., Ishikawa, T. & Noyori, R. (1997) Chemical implication for antitumor antiviral prostaglandins: reaction of Δ^7-prostaglaindin A_1 and prostaglandin A_1 methyl esters with thiol. *J. Am. Chem. Soc.*, **119**, 2376–2385.

Tanikawa, M., Yamada, K., Tominaga, K., Morisaki, H., Kaneko, Y., Ikeda, K., Suzuki, M., Kiho, T., Tomokiyo, K., Furuta, K., Noyori, R. & Nakanishi, M. (1998) Potent prostaglandin A_1 analogs that suppress tumor cell growth through induction of p21 and reduction of cyclin E. *J. Biol. Chem.*, **273**, 18522–18527.

Yet, S.F., Perrella, M.A., Layne, M.D., Hsieh, C.M., Maemura, K., Kobik, L., Wiesel, P., Christou, H., Kourembanas, S. & Lee, W.S. (1999) Hypoxia induces severe right ventricular dilatation and infarction in heme oxygenase-1 null mice. *J. Clin. Invest.*, **103**, R23–R29.

Zakhary, R., Poss, K.D., Jaffrey, S.R., Ferris, C.D., Tonegawa, S. & Snyder, S.H. (1997) Targeted gene deletion of heme oxygenase 2 reveals neuronal role for carbon monoxide. *Proc. Natl Acad. Sci. USA*, **94**, 14848–14853.

Available online at www.sciencedirect.com
SCIENCE DIRECT®
ELSEVIER
Gene 310 (2003) 17–28
GENE
AN INTERNATIONAL JOURNAL ON GENES AND GENOMES
www.elsevier.com/locate/gene

Characterization of the mouse *Abcc12* gene and its transcript encoding an ATP-binding cassette transporter, an orthologue of human ABCC12☆

Hidetada Shimizu[a], Hirokazu Taniguchi[b], Yoshitaka Hippo[b], Yoshihide Hayashizaki[c], Hiroyuki Aburatani[b], Toshihisa Ishikawa[a,*]

[a]*Department of Biomolecular Engineering, Graduate School of Bioscience and Biotechnology, Tokyo Institute of Technology, Nagatsuta 4259, Midori-ku, Yokohama 226-8501, Japan*
[b]*Genome Science Division, Research Center for Advanced Science and Technology, The University of Tokyo, 4-6-1 Komaba, Meguro-ku, Tokyo 153-8904, Japan*
[c]*Genome Exploration Research Group, Genome Science Laboratory, Genome Sciences Center, RIKEN, 1-7-22 Suehiro-cho, Tsurumi-ku, Yokohama 230-0045, Japan*

Received 13 December 2002; received in revised form 24 February 2003; accepted 6 March 2003
Received by T. Gojobori

Abstract

We have recently reported on two novel human ABC transporters, ABCC11 and ABCC12, the genes of which are tandemly located on human chromosome 16q12.1 [Biochem. Biophys. Res. Commun. 288 (2001) 933]. The present study addresses the cloning and characterization of Abcc12, a mouse orthologue of human ABCC12. The cloned Abcc12 cDNA was 4511 bp long, comprising a 4101 bp open reading frame. The deduced peptide consists of 1367 amino acids and exhibits high sequence identity (84.5%) with human ABCC12. The mouse *Abcc12* gene consists of at least 29 exons and is located on the mouse chromosome 8D3 locus where conserved linkage homologies have hitherto been identified with human chromosome 16q12.1. The mouse *Abcc12* gene was expressed at high levels exclusively in the seminiferous tubules in the testis. In addition to the Abcc12 transcript, two splicing variants encoding short peptides (775 and 687 amino acid residues) were detected. In spite of the genes coding for both ABCC11 and ABCC12 being tandemly located on human chromosome 16q12.1, no putative mouse orthologous gene corresponding to the human *ABCC11* was detected at the mouse chromosome 8D3 locus.

Keywords: ATP binding cassette transporter; Mouse; Abcc12; Mouse chromosome 8; Human chromosome 16; Sertoli cell

1. Introduction

The ATP-binding cassette (ABC) transporters form one of the largest protein families and play a biologically important role as membrane transporters or ion channel modulators (Higgins, 1992). According to the recently published draft sequence of the human genome, more than 50 human ABC transporter genes (including pseudogenes[1]) are anticipated to exist in the human genome. Hitherto 49 human ABC-transporter genes have been identified and sequenced (recent reviews: Klein et al., 1999; Dean et al., 2001; Borst and Oude Elferink, 2002). Based on the arrangement of their molecular structural components, i.e. the nucleotide binding domain and the topology of transmembrane spanning domains, human ABC transporters are classified into seven different gene families designated as A to G (the new nomenclature of human ABC transporter genes: http://gene.ucl.ac.uk/nomenclature/genefamily/abc.html). Mutations in the human ABC transporter genes have been reported to cause such genetic diseases as Tangier

☆ The cDNA sequences of mouse Abcc12 and its splice variants A and B have been registered in GenBank under the accession numbers of AF502146 (April 12, 2002), AF514414 (May 22, 2002), and AF514415 (May 22, 2002), respectively.

Abbreviations: ABC, ATP-binding cassette; EST, expresed sequence tag; MRP, multidrug resistance-associated protein; GAPDH, glutaraldehyde dehydrogenase; GS-X, pump, ATP-dependent glutathione *S*-conjugate export pump; RT–PCR, reverse transcriptase–polymerase chain reaction.

* Corresponding author. Tel.: +81-45-924-5800; fax: +81-45-924-5838.
E-mail address: tishikaw@bio.titech.ac.jp (T. Ishikawa).

[1] A truncated human ABC transporter, ABCC13 (GenBank accession number: AF418600), has most recently been cloned (Yabuuchi et al., 2002).

0378-1119/03/$ - see front matter © 2003 Elsevier Science B.V. All rights reserved.
doi:10.1016/S0378-1119(03)00504-3

disease, cystic fibrosis, Dubin–Johnson syndrome, Stargardt disease, and sitosterolemia (recent reviews: Dean et al., 2001; Borst and Oude Elferink, 2002).

We originally reported that transport of glutathione S-conjugates and leukotriene C_4 (LTC_4) across the cell membrane is mediated by an ATP-dependent transporter named the 'GS-X pump' (Ishikawa, 1989, 1992); however, the molecular nature of the transporter was not uncovered at that time. Later studies have provided evidence that the GS-X pump is encoded, at least, by the ABCC1 (MRP1) gene (Leier et al., 1994; Müller et al., 1994). ABCC1 (MRP1) was first identified by Cole et al. (1992) in the molecular cloning of cDNA from human multidrug-resistant lung cancer cells. After the discovery of the ABCC1 (MRP1) gene, six human homologues, ABCC2 (cMOAT/MRP2), ABCC3 (MRP3), ABCC4 (MRP4), ABCC5 (MRP5), ABCC6 (MRP6), and ABCC10 (MRP7) have been successively identified. Those ABC transporters exhibit a wide spectrum of biological functions and are involved in the transport of drugs as well as endogenous substances (see recent reviews: Borst and Oude Elferink, 2002; Ishikawa, in press).

Most recently, our group (Yabuuchi et al., 2001) and others (Tammur et al., 2001; Bera et al., 2001, 2002) have independently discovered two novel ABC transporters, human ABCC11 (MRP8) and ABCC12 (MRP9), that belong to the ABCC gene family. The predicted amino acid sequences of both gene products show a high similarity with ABCC5. The *ABCC11* and *ABCC12* genes consist of at least 30 and 29 exons, respectively, and they are tandemly located in a tail-to-head orientation on human chromosome 16q12.1 (Yabuuchi et al., 2001; Tammur et al., 2001). The physiological functions of these genes are not yet known; however recent linkage analyses have demonstrated that a putative gene responsible for paroxysmal kinesigenic choreoathetosis (PKC), a genetic disease of infancy, is located in the region of 16p11.2–q12.1 (Lee et al., 1998; Tomita et al., 1999). Since the *ABCC11* and *ABCC12* genes are encoded at that 16q12.1 locus, a potential link between the PKC gene and these ABC transporters has been implicated.

To elucidate the physiological function of human ABCC11 and ABCC12, knockout mice are considered to be a useful animal model. For this reason, we have undertaken the present study to pursue mouse orthologues of ABCC11 and ABCC12. In this study, we have cloned the cDNA of mouse Abcc12 and characterized its chromosomal location, gene organization, tissue-specific expression, the putative protein structure, and splicing variants.

2. Materials and methods

2.1. Cloning of mouse Abcc 12 cDNA

Mouse EST clones bearing a high similarity to partial sequences of human ABCC 12 cDNA were extracted from the NCBI mouse EST database and the mouse cDNA 'FANTOM 2' database of RIKEN (The FANTOM Consortium, 2002) by using the NCBI BLAST search program (Fig. 1). We have screened multiple tissue cDNA libraries (MTC, Clontech, Palo Alto, CA, USA) by PCR with the following primers deduced from the EST sequences: the forward primer, 5′-AGTTCCCTCATTTCAGCTCTCC-TAGGAC-3′, and the backward primer, 5′-GCAGGTA-GAGCTGACGATTAGCATAC-3′. High expression was detected in mouse testis.

To clone the mouse Abcc12 cDNA from the testis, we have designed four sets of PCR primers, as shown in Fig. 1. The PCR primer sets were as follows: c12-1 (the forward primer: 5′-GCCAAAAGTCGAGGGCTCCAAAACACC-3′ and the backward primer: 5′-GGCCACTGCTTTGACC-GAGAA-3′), c12-2 (the forward primer: 5′-GGCTGGC-TATGTCCAAAGTGGAA-3′ and the backward primer: 5′-GATGCCAAACATCAACACAGACACC-3′), c12-3 (the forward primer: 5′-GATGATGGGCAGCTCTGCTT-TC-3′ and the backward primer: 5′-TCACATGTCCA-TCGCCTCCTCTCA-3′), and c12-4 (the forward primer: 5′- GCCCGACTCTGCATTTGCGA-3′ and the backward primer: 5′-CAAAATCCAGGAACGCTGTCATCTCC-3′). The PCR reaction was performed with mouse testis cDNA (Clontech) and *Ex Taq* polymerase (TaKaRa, Japan), where the reaction consisted of 30 cycles of 95 °C for 30 s, 58 °C for 30 s, and 72 °C for 90 s. After agarose gel electrophoresis, the PCR products were extracted from the gels and subsequently inserted into TA cloning vectors (Invitrogen, Japan). The sequences of the inserts were analyzed with an automated DNA sequencer. (Toyobo Gene Analysis, Japan). The whole cDNA of mouse Abcc12 was obtained by assembling those partial sequences.

2.2. Detection of mouse Abcc 12 transcripts by PCR in different tissues

The expression of mouse Abcc 12 in different organs was examined by PCR with the mouse Multiple Tissue cDNA (MTC, Clontech). Two sets of PCR primers were designed to detect the corresponding transcript (Fig. 1), namely, the primer set #1 detecting the 5′-part of Abcc12 cDNA (the forward primer: 5′-CCACTGTCTCCTTATGACTCATCG-GAC-3′, the backward primer: 5′-GGGACAAAACAAGG-CAGCCTCAAAC-3′) and the primer set #2 recognizing the 3′-part of Abcc12 cDNA (the forward primer: 5′-TAT-GGCCCGGGCACTTCTCCGTAA-3′, the backward primer 5′-GACCTTTACAGTCCAACCTCTGCAGCTAGT-3′). The PCR reaction consisted of 35 cycles of 95 °C for 30 s, 58 °C for 30 s, and 72 °C for 30 s. The reaction products were detected by agarose gel electrophoresis.

2.3. Northern blot analysis

Mouse organs (i.e. heart, kidney, brain, testis, spleen, stomach, liver, thymus, and small intestine) were surgically

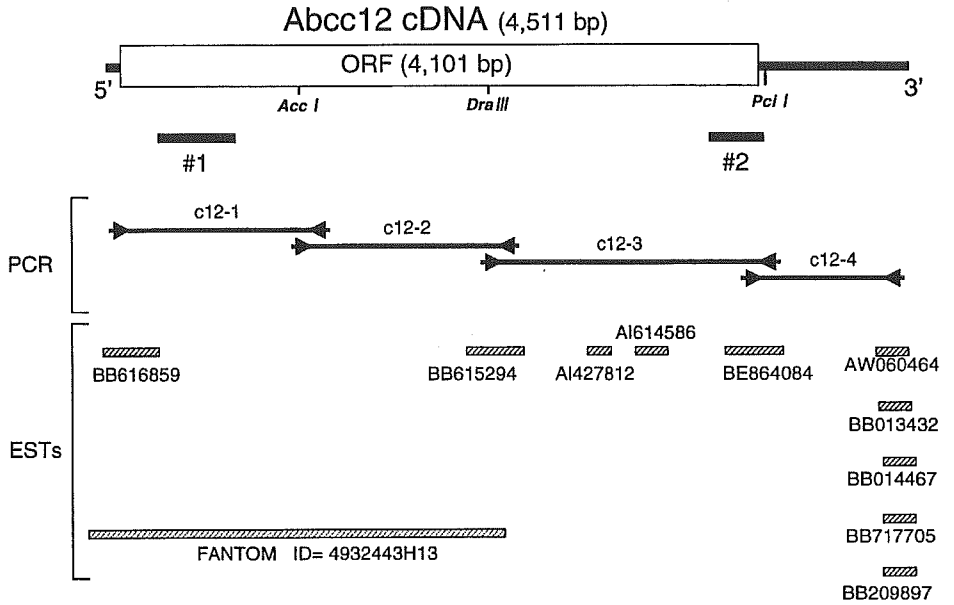

Fig. 1. Strategy for the cloning of mouse Abcc12 cDNA. The open reading frame (ORF) is indicated by a box. The cleavage sites by restriction enzymes (*Acc* I, *Dra* III and *Pci* I) are also indicated. The cDNA was cloned by PCR with four sets of primers, c12-1, c12-2, c12-3, and c12-4, as described in Section 2. The forward and backward PCR primers are indicated by arrows, and the resulting PCR products are represented by straight lines. ESTs and the FANTOM 2 cDNA are sorted according to the sequence homology with Abcc12 cDNA. PCR products used to detect the Abcc12 transcript in different tissues are indicated by #1 and #2.

excised from Balb/C mice (10 weeks old) under anesthesia and immediately frozen in liquid nitrogen. The tissue was pulverized in a mortar containing liquid nitrogen. The resulting tissue powder was subsequently homogenized in TRIzol (Invitrogen, Japan) by using a Polytron homogenizer, and total RNA was extracted according to the manufacturer's protocol. A sample (15 μg/lane as determined by absorbance at 260 nm) of RNA, thus prepared, was subjected to electrophoresis in 1% (w/v) agarose gels containing formaldehyde and then transferred to Hybond-XL membranes (Amersham Pharmacia Biotech). RNA was fixed on the membrane surface by baking at 80 °C for 2 h.

Three different DNA probes encoding partial sequences (463–1165; 1440–2116; 3660–4154) of the Abcc12 cDNA ORF were prepared and separately labeled with [^{32}P]dCTP by using the BcaBest labeling kit (TaKaRa) according to the random-primed labeling method. Hybridization with those DNA probes was carried out according to the hybridization protocol of the Expresshybri kit (Clontech), and the hybridization signal was detected in a BASS 2000 (Fuji Film, Japan).

2.4. Laser-captured microdissection and RT–PCR

The frozen tissue of mouse testis was cut into thin sections (5 μm thickness) with a microtome (Leika GmbH, Germany) and mounted onto glass slides. The tissue slice on the glass slide was stained in 70% Giemsa solution. After staining, the tissue slices were dehydrated in 100% ethanol and subsequently in 100% xylene. The slide was air-dried, and the seminiferous tubules and the interstitium in the tissue slices were excised by laser-capture microdissection with an Arcturus PixCell 2 LCM system (Arcturus Engineering, Mountain View, CA). The dissected samples were homogenized in 200 μl of TRIzol, and RNA was extracted. mRNA was then converted to cDNA by reverse transcriptase (RT) using a SensiScripts kit (Qiagen). Expression of mouse Abcc12 in these samples was detected by PCR with the same primers and under the same conditions as described in Section 2.2.

2.5. In situ hybridization

The testis was surgically excised from mice under anesthesia and immersed in phosphate-buffered saline (PBS) containing 4% paraformaldehyde. The tissue was embedded in paraffin, and thin sections (4 μm thickness) were prepared with a microtome. The resulting thin sections were soaked in xylene three times (3 min for each) and twice in 100% ethanol (3 min for each). Thereafter, sections were rinsed in 70% ethanol and subsequently in 0.1% DEPC-treated water three times. Prior to hybridization, the sections were treated with proteinase K (1:400 v/v) in Tris-buffered saline (TBS) at room temperature for 10 min and

A

```
Mouse Abcc12    1 MVGEGPYLISDLDRRGHRRSFAERYDPSLKTMIPVRPRARLAPNPVDDAGLLSFATFSWL 60
Human ABCC12    1 MVGEGPYLISDLDQRGRRRSFAERYDPSLKTMIPVRPCARLAPNPVDDAGLLSFATFSWL 60

Mouse Abcc12   61 TPVMIRSYKHTLTVDTLPPLSPYDSSDINAKRFQILWEEEIKRVGPEKASLGRVVWKFQR 120
Human ABCC12   61 TPVMVKGYRQRLTVDTLPPLSTYDSSDTNAKRFRVLWDEEVARVGPEKASLSHVVWKFQR 120

Mouse Abcc12  121 TRVLMDVVANILCIVMAALGPTVLIHQILQHITSISSGHIGIGICLCLALFTTEFTKVLF 180
Human ABCC12  121 TRVLMDIVANILCIIMAAIGPTVLIHQILQQTERTSG-KVWVGIGLCIALFATEFTKVFF 179

Mouse Abcc12  181 WALAWAINYRTAIRLKVALSTLIFENLLSFKTLTHISAGEVLNILSSDSYSLFEAALFCP 240
Human ABCC12  180 WALAWAINYRTAIRLKVALSTLVFENLVSFKTLTHISVGEVLNILSSDSYSLFEAALFCP 239

Mouse Abcc12  421 PPSYITQPEDPDTILLLANATLTWEQEINRKSDPPKAQIQKRHVFKKQRPELYSEQSRSD 480
Human ABCC12  420 PPSYITQPEDPDTVLLLANATLTWEHEARQESTPKKLQNQKRHLCKKQRSEAYSERSPPA 479
                                                Walker A
Mouse Abcc12  481 QGVASPEWQSGSPKSVLHNISFVVRKGKVLGICGNVGSGKSSLISALLGQMQLQKGVVAV 540
Human ABCC12  480 KGATGPEEQSDSLKSVLHSISFVVRKGKILGICGNVGSGKSSLLAALLGQMQLQKGVVAV 539

Mouse Abcc12  541 NGPLAYVSQQAWIFHGNVRENILFGEKYNHQRYQHTVHVCGLQKDLNSLPYGDLTEIGER 600
Human ABCC12  540 NGTLAYVSQQAWIFHGNVRENILFGEKYDHQRYQHTVRVCGLQKDLSNLPYGDLTEIGER 599
                  Signature C      Walker B
Mouse Abcc12  601 GVNLSGGQRQRISLARAVYANRQLYLLDDPLSAVDAHVGKHVFEECIKKTLKGKTVVLVT 660
Human ABCC12  600 GLNLSGGQRQRISLARAVYSDRQLYLLDDPLSAVDAHVGKHVFEECIKKTLRGKTVVLVT 659

Mouse Abcc12  661 HQLQFLESCDEVILLEDGEICEKGTHKELMEERGRYAKLIHNLRGLQFKDPEHIYNVAMV 720
Human ABCC12  660 HQLQFLESCDEVILLEDGEICEKGTHKELMEERGRYAKLIHNLRGLQFKDPEHLYNAAMV 719

Mouse Abcc12  721 ETLKESPAQRDEDAVLASGDEKDEGKEPETEE-FVDTNAPAHQLIQTESPQEGIVTWKTY 779
Human ABCC12  720 EAFKESPAEREEDAVLAPGNEKDEGKESETGSEFVDTKVPEHQLIQTESPQEGTVTWKTY 779

Mouse Abcc12  780 HTYIKASGGYLVSFLVLCLFFLMMGSSAFSTWWLGIWLDRGSQVVCASQNNKTACNVDQT 839
Human ABCC12  780 HTYIKASGGYLLSLFTVFLFLLMIGSAAFSNWWLGLWLDKGSRMTCGPQGNRTMCEVGAV 839

Mouse Abcc12  840 LQDTKHHMYQLVYIASMVSVLMFGIIKGFTFTNTTLMASSSLHNRVFNKIVRSPMSFFDT 899
Human ABCC12  840 LADIGQHVYQRVYTASMVFMLVFGVTKGFVFTKTTLMASSSLHDTVFDKILKSPMSFFDT 899

Mouse Abcc12  900 TPTGRLMNRFSKDMDELDVRLPFHAENFLQQFFMVVFILVIMAAVFPVVLVVLAGLAVIF 959
Human ABCC12  900 TPTGRLMNRFSKDMDELDVRLPFHAENFLQQFFMVVFILVILAAVFPAVLLVVASLAVGF 959

Mouse Abcc12  960 LILLRIFHRGVQELKQVENISRSPWFSHITSSIQGLGVIHAYDKKDDCISKFKTLNDENS 1019
Human ABCC12  960 FILLRIFHRGVQELKKVENVSRSPWFTHITSSMQGLGIIHAYGKKESCIT-Y-------- 1010

Mouse Abcc12 1020 SHLLYFNCALRWFALRMDILMNIVTFVVALLVTLSFSSISASSKGLSLSYIIQLSGLLQV 1079
Human ABCC12 1011 -HLLYFNCALRWFALRMDVLMNILTFTVALLVTLSFSSISTSSKGLSLSYIIQLSGLLQV 1069

Mouse Abcc12 1080 CVRTGTETQAKFTSAELLREYILTCVPEHTHPFKVGTCPKDWPSRGEITFKDYRMRYRDN 1139
Human ABCC12 1070 CVRTGTETQAKFTSVELLREYISTCVPECTHPLKVGTCPKDWPSCGEITFRDYQMRYRDN 1129
                                Walker A
Mouse Abcc12 1140 TPLVLDGLNLNIQSGQTVGIVGRTGSGKSSLGMALFRLVEPASGTIIIDEVDICTVGLED 1199
Human ABCC12 1130 TPLVLDSLNLNIQSGQTVGIVGRTGSGKSSLGMALFRLVEPASGTIFIDEVDICILSLED 1189

Mouse Abcc12 1200 LRTKLTMIPQDPVLFVGTVRYNLDPLGSHTDEMLWHVLERTFMRDTIMKLPEKLQAEVTE 1259
Human ABCC12 1190 LRTKLTVIPQDPVLFVGTVRYNLDPFESHTDEMLWQVLERTFMRDTTMKLPEKLQAEVTE 1249
                  Signature C      Walker B
Mouse Abcc12 1260 NGENFSVGERQLLCMARALLRNSKIILLDEATASMDSKTDTLVQSTIKEAFKSCTVLTIA 1319
Human ABCC12 1250 NGENFSVGERQLLCVARALLRNSKIILLDEATASMDSKTDTLVQNTIKDAFKGCTVLTIA 1309

Mouse Abcc12 1320 HRLNTVLNCDLVLVMENGKVIEFDKPEVLAEKPDSAFAMLLAAEVGL 1366
Human ABCC12 1310 HRLNTVLNCDHVLVMENGKVIEFDKPEVLAEKPDSAFAMLLAAEVRL 1356
```

Fig. 2. Alignments of the mouse Abcc12 and human ABCC12 proteins. (A) Amino acid sequences were aligned by using the GENETYX-MAC program. The Walker A and B motifs as well as the signature C are indicated by boxes. (B) The hydropathy plots of mouse Abcc12 (this study) and human ABCC12 (Yabuuchi et al., 2001). The hydropathy profiles were calculated according to the Kyte and Doolittle (1982) algorithm.

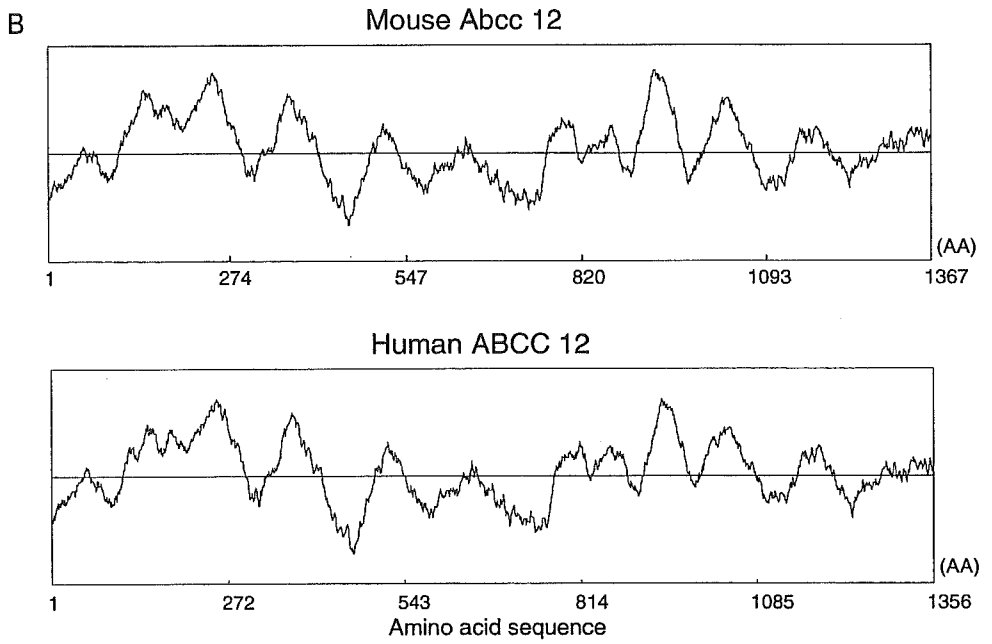

Fig. 2 (*continued*)

then rinsed with 0.1% DEPC-treated water. The following biotin-labeled oligonucleotide DNA probes were synthesized, i.e. the sense probe: 5′-AGCCTGACTCTGCATTTGCGATGTTACTAGCTGCAG-3′ and the anti-sense probe: 5′-CTGCAGCTAGTAACATCGCAAATGCAGAGTCAGGCT-3′. The probes were diluted in the DAKO in situ hybridization solution (DAKO S3304) at a final concentration of 1 ng/ml. The hybridization with the sense or the anti-sense probe was carried out on the thin section at 37 °C overnight. Thereafter, the slides were incubated in 0.1× SSC (300 mM sodium chloride and 1.5 mM sodium citrate, pH 7.0) at 37 °C for 20 min twice and washed in TBS at room temperature for 3 min.

In situ hybridization signals were visualized by a tyramide amplification signal detection system using the DAKO GenPoint system (DAKO K0620), according to manufacturer's instructions. Finally, the sections were counterstained with Mayer's hematoxylin (Sigma, USA).

2.6. Data analysis

DNA sequences were analyzed with the GENETYX-MAC software ver.11 and compared with other ABCC transporter genes registered in the NCBI database. The hydropathy profile of the protein deduced from the cDNA sequence was calculated with the Kyte and Doolittle hydropathy algorithm (Kyte and Doolittle, 1982), and the SOSUI program (http://sosui.proteome.bio.tuat.ac.jp/sosuimenu0.html) was used to predict transmembrane domains. Phylogenic relationships were calculated by using the distance-based neighbor-joining method (Saitou and Nei, 1987).

3. Results

3.1. Cloning and characterization of mouse Abcc 12 cDNA

Fig. 1 depicts the strategy of cloning mouse Abcc12 cDNA. The sequence of human ABCC12 cDNA was applied to the currently available mouse EST database on an NCBI BLAST search to discover ESTs encoding partial sequences of mouse Abcc 12. Thereby, the following EST clones were extracted: BB616859, BB615294, AI427812, AI614586, BE864084, AW060464, BB013432, BB014467, BB717705, and BB209897. In addition, in a search of the FANTOM 2 database of RIKEN, we found one cDNA clone (ID number = 4932443H13) that exhibited a high sequence homology with human ABCC12 cDNA. Based on those ESTs as well the partial cDNA clone (ID = 4932443H13), we designed four sets of PCR primers to clone the mouse Abcc12 cDNA (see Section 2 for experimental details). By PCR, we obtained a total of four cDNA fragments (Fig. 1) and assembled them to construct the full cDNA encoding mouse Abcc12.

Table 1
Amino acid sequence identity of the mouse Abcc 12 with human ABC proteins in the ABCC sub-family

ABC protein	Identity (%)
ABCC1	33.4
ABCC2	32.1
ABCC3	31.1
ABCC4	40.2
ABCC5	43.7
ABCC6	28.5
CFTR (ABCC7)	27.9
ABCC8	30.6
ABCC9	27.9
ABCC10	34.6
ABCC11	47.8
ABCC12	84.5

The amino acid sequences of human ABC proteins were acquired from the NCBI database (refer to the accession numbers given in the legend of Fig. 3).

3.2. Characterization of mouse Abcc12 cDNA in comparison with members of the human ABCC sub-family

The cloned mouse Abcc12 cDNA (GenBank accession number: AF502146) was 4511 bp long, containing a 4101 bp open reading frame (ORF). The Abcc12 cDNA has a Kozak consensus initiation sequence (Kozak, 1991) for translation around the first ATG region, namely, 5′-ATCAAG**ATG**G-3′. The amino acid sequence deduced from the cDNA sequence with the GENETYX-MAC program revealed that the cDNA encodes a single peptide consisting of 1366 amino acid residues (Fig. 2A). Motif analysis predicted the existence of two sets of ATP-binding cassettes (Walker et al., 1982): namely, Walker A (amino acids 514–521 and 1161–1168), Walker B (amino acids 624–628 and 1284–1288), and signature C motifs (amino acids 604–618 and 1264–1278) (Fig. 2A). Fig. 2B shows the hydropathy plots of mouse Abcc12 and human ABCC12, demonstrating a remarkable similarity between these transporters.

Table 1 shows that the amino acid sequence of mouse Abcc12 has the highest identity with human ABCC12 among the hitherto known members of the human ABCC sub-family. The sequence identity of mouse Abcc12 with human ABCC12 was 84.5%, whereas its identity with human ABCC11 was 47.8%. The identity of mouse Abcc12 with other human members was relatively low, in the range of 27.9 to 43.7% (Table 1).

Fig. 3 shows the phylogenic relationship among the members of the human and mouse ABCC subfamily. Mouse Abcc12, as well as human ABCC12, apparently belongs to a cluster named 'Class D' that comprises ABCC4, ABCC5, ABCC11, Abcc4, and Abcc5 (see Section 4 for the classification).

3.3. Chromosomal location of the mouse Abcc 12 gene

Fig. 4 shows the location of the *Abcc12* gene on the mouse chromosome 8. The mouse Abcc12 gene spans a 65 kb length and is located between two microsatellite markers, D8Mit347 and D8Mit348, at the D3 region of the mouse chromosome 8 (Fig. 4), as referred to in the mouse genome databases of NCBI and EMBL/UCSC (Mouse Genome Sequencing Consortium, 2002). This genome region of the mouse chromosome 8 is reportedly related to human chromosome 16q12.1, where the human *ABCC11* and *ABCC12* genes are tandemly located (Yabuuchi et al., 2001; Tammur et al., 2001). Comparison of the cloned

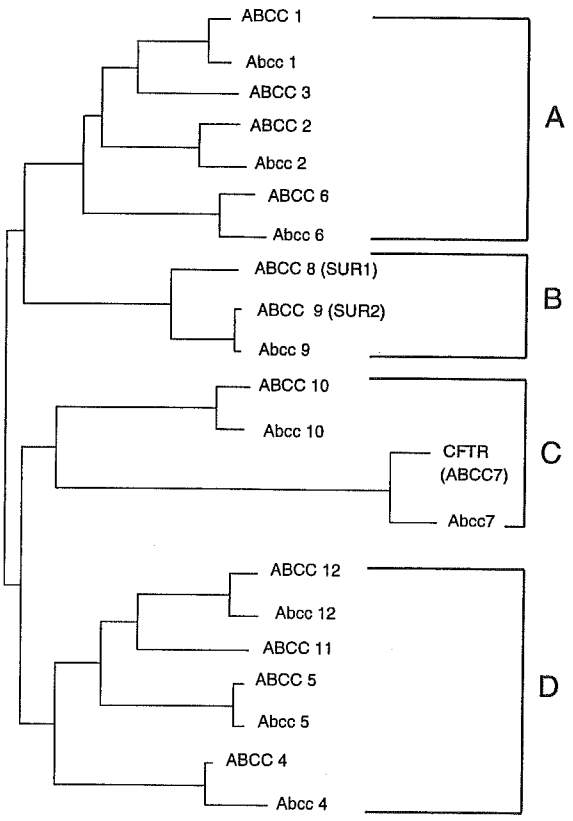

Fig. 3. The phylogenetic relationship among hitherto characterized members of the human and mouse ABCC sub-family. The phylogenetic distance was calculated according to the distance-based neighbor-joining method (Saitou and Nei, 1987). For the sequences of those ABC transporters, accession numbers are as follows: human ABCC1 (NM004996), ABCC2 (NM000392), ABCC3 (Y17151), ABCC4 (NM005845), ABCC5 (NM005688), ABCC6 (NM001171), ABCC7 (NM000492), ABCC8 (NM000352), ABCC9 (NM005691), ABCC10 (AK000002), ABCC11 (AF367202), ABCC12 (NM033226) mouse Abcc1 (NM008576), Abcc2 (NM013806), Abcc4 (D630049P08), Abcc5 (NM013790), Abcc6 (NM018795), Abcc7 (NM021050), Abcc8 (XM133448), Abcc9 (NM011511), Abcc10 (AF406642), Abcc12 (AF502146).

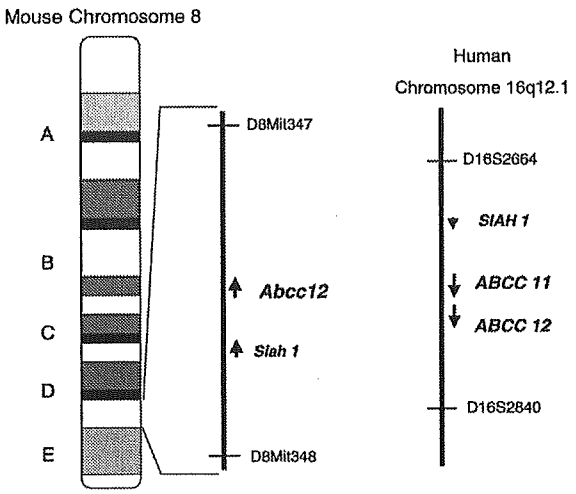

Fig. 4. Location of the *Abcc12* gene on mouse chromosome 8. *Abcc12* and *Siah 1* genes are located in the mouse chromosomal region between two microsatellite markers, D8Mit347 and D8Mit348. Human *ABCC11*, *ABCC12*, and *SIAH 1* genes are located in the region between D16S2664 and D16S2840 on the human chromosome 16q12.1.

Abcc12 cDNA with the mouse genome data revealed that the *Abcc12* gene consists of at least 29 exons, where the translation start codon (ATG) was found in exon 1. In addition, two sets of ATP-binding cassettes were detected. The first Walker A motif is located in the exon 10, whereas the second Walker A motif spreads over exons 24 and 25. Two Walker B motifs are encoded in exons 13 and 28, and two signature C motifs are located in exons 13 and 27.

Table 2 summarizes the exon and intron boundaries with partial sequences at each splicing site of the *Abcc12* gene; however, the partial sequences of the introns proximal to both 5′- and 3′-ends of exon 3 are presently not available (Table 2). These results suggest that the splicings of the mouse Abcc12 gene follow the conventional GT–AG rule, except for the exon 19.

3.4. Tissue-dependent expression of the mouse Abcc 12 gene

Fig. 5A shows the expression levels of the mouse Abcc12 gene in different organs as detected by RT–PCR with two different sets of PCR primers #1 and #2 (see Fig. 1 and Section 2 for details). The products of PCR reactions with primers #1 and #2 were 486 and 288 bp, respectively. Among the organs tested, the highest expression (mRNA) of

Table 2
Partial sequences of intron/exon and exon/intron boundaries in the mouse *Abcc 12* gene

Exon	Size (bp)	Intron/Exon		Exon/Intron	
1	152	tgtcccgaag	CCAAGAGTCG	CCCGTGCAAG	gtgagccagg
2	156	tttgctctag	GTTGGCACCC	ACGCCAAGAG	gtaccaggct
3[a]	147	nnnnnnnn	ATTCCAGATC	CTTGGGGCCG	nnnnnnnn
4	238	tgttttacag	ACAGTTCTCA	TGCAGGCGAG	gtaagcaggg
5	174	ttcttttctag	GTACTCAATA	CCCGATCCAG	gtaagttggg
6	148	tcgatttcag	ATGTTTATGG	ACCATTCACG	gtaagatgag
7	149	tcttttgcag	ACATAAGAAA	TGCCCCTGTG	gtaagagtta
8	108	cctccttcag	GCATTTAGTG	GAGAATGAAG	gtataagtaa
9	279	ttaatctcag	AAAATCCTCA	GGTGAGAAAG	gtgagtgtat
10	72	tctctgacag	GGGAAGGTCT	CCTAGGACAG	gtgagtgtgt
11	125	atcgctctag	ATGCAGTTAC	ACCACCAAAG	gtattattaa
12	73	atgtctacag	GTACCAACAC	CCTGACTGAG	gtaagcagag
13	204	ctgtccacag	ATTGGAGAGC	CCAGTTGCAG	gtgactggga
14	135	gtctctgcag	TTCCTGGAGT	GCAATTCAAG	gtaaactgca
15	76	ttatctccag	GATCCAGAGC	GAAGACGCTG	gtacagtcag
16	69	ctcatcctag	TCTTGGCTTC	GACACAAACG	gtatttacca
17	90	gtctctgcag	CTCCCGCTCA	GCTTCTGGAG	gtttagtata
18	104	tctccggcag	GGTACCTGGT	GGGTTCCCAG	gtgagtttcc
19	194	tgtgttgcag	GTCGTCTGTG	GAGTATTTAATA	caaggtagaa
20	229	ttctaccctc	AGATCGTCAG	TTCTTTTACG	gtaggattat
21	138	tcccccacag	CATCTTCCAT	GCATCAGCAA	gtgagtggat
22	187	ttgactttag	GTTTAAGACA	CATCATCCAG	gtaacggctg
23	90	ttcccaacag	CTCAGTGGAT	GTACATTTTG	gtaaggaatg
24	190	tgcttttcag	ACCTGTGTTC	ACGGGCTCCG	gtgaggacag
25	160	ttgtccccag	GAAAATCATC	GTACAGTAAG	gtagctgttt
26	79	ttcgttgcag	GTACAACTTG	GAGAGACACA	gtacgtcttg
27	114	tgttttatag	ATAATGAAAC	TAATTCAAAA	gtaaggaaac
28	165	tccttaacag	ATCATTCTCC	AAATGGGAAG	gtgcaggaaa
29	464	tgattttcag	GTGATTGAGT	CCTGGATTTT	gttaccagac

[a] The partial sequences of the introns proximal to the 5′- and 3′-ends of exon 3 are not available, therefore they are represented by 'nnnn'.